Geomorphology 494 (2026) 110101

Contents lists available at ScienceDirect

Geomorphology

journal homepage: www.journals.elsevier.com/geomorphology

Stream channel morphology and water flow in ice-free areas of Byers Peninsula, South Shetland Islands, Antarctica

José Antonio Ortega-Becerril [a,*], Thomas Schmid [b], Juan Pablo Corella [c], Luis Carcavilla [d], Mikel Calle [e,f], Jerónimo López-Martínez [a]

[a] Facultad de Ciencias, Universidad Autónoma de Madrid, Campus de Cantoblanco, 28049, Madrid, Spain
[b] Department of Environment, Centro de Investigaciones Energéticas, Medioambientales y Tecnológicas (CIEMAT), Avenida Complutense, 40, 28040, Madrid, Spain
[c] Museo Nacional de Ciencias Naturales, Consejo Superior de Investigaciones Científicas (CSIC), Serrano, 115 bis, 28006, Madrid, Spain
[d] Instituto Geológico y Minero de España (IGME-CSIC), Calera, 1, 28760, Tres Cantos, Madrid, Spain
[e] Facultad de Ciencias Geológicas, Universidad Complutense de Madrid, C/ José Antonio Novais, 12, Ciudad Universitaria, 28040, Madrid, Spain
[f] University of Turku, Geography and Geology Department, FI-20014, Turun yliopisto, Turku, Finland

ARTICLE INFO

Keywords:
Fluvial geomorphology
Drainage system morphometry
Geomorphological evolution
Antarctic Peninsula region

ABSTRACT

Fluvial stream channels in Antarctic ice-free areas provide valuable insights into deglaciation/neoglaciation, and the pace of morphogenetic processes shaping the landscape. The northern Antarctic Peninsula, particularly the South Shetland Islands, offers unique conditions for such studies due to extensive ice-free zones, glacial history, and rapidly changing environments. This research focuses on Byers Peninsula (BP), the largest ice-free area of the archipelago, characterized by a well-developed drainage system previously studied and mapped. This paper expands knowledge of channel development, water flow, and related morphologies, relevant for understanding other ice-free Antarctic regions. Morphometric analyses were conducted on 26 streams, alongside evaluation of channel equilibrium in three selected watersheds. Water flow was monitored for two years in two streams using data loggers, with complementary field data from a third. Seven morphotypes were distinguished within a theoretical watershed, including diffuse drainage, platform lakes, braided systems, canyons, cutting raised platforms, open braided channels, entrenched channels on raised beaches, lagoons and/or small fans. Results highlight significant variability in channel size and hydraulic properties across sub-basins. Southern BP streams reveal higher fluvial energy, while Western streams, draining larger basins with higher stream orders, display more advanced fluvial development and concentrate the main systems of the region. Basin orientation, glacier proximity, and topography emerged as key factors shaping channel dimensions, while glacial lake outburst floods strongly influenced morphology and sediment dynamics. The presence of paired morphometrically similar channels on North and South coasts supports a stepwise west–east retreat of Rotch Dome Glacier, marked by stagnation phases producing mature channels and rapid retreats yielding less developed systems.

1. Introduction

Ice-free areas in Antarctica comprise about 0.3 % of the total surface and play a crucial role in the region's biodiversity and ecosystem functioning (Convey et al., 2014). They offer insights into the Antarctic geological and geomorphological evolution and into the environmental conditions. These areas are key to determine contemporary geomorphological processes, such as periglacial and paraglacial dynamics, coastal changes and landscape evolution after glacial retreat (Zwoliński, 2007; López-Martínez et al., 2012). The study of the ice-free areas allows us to consider climate records preserved in exposed rocks, sediments and soils, and to understand the evolution of the recent landscape and surface processes (Palacios et al., 2020). These areas can provide crucial information about past and current conditions, as well as about possible occurrences and consequences of future environmental changes. The northern Antarctic Peninsula (AP) region and especially within the South Shetland Islands (SSI) are relevant to study processes affecting the ice-free areas due to the past and current environmental changes under a maritime climate. This paper focuses on Byers Peninsula (BP) that is the largest ice-free area in the archipelago.

Glacier retreat and advances in the SSI provided a significant quantity of melted water and energy to reshape the landscape within ice-free

* Corresponding author.
E-mail addresses: j.ortega@uam.es, jortega47@yahoo.com (J.A. Ortega-Becerril).

https://doi.org/10.1016/j.geomorph.2025.110101
Received 30 September 2025; Received in revised form 19 November 2025; Accepted 20 November 2025
Available online 22 November 2025

areas during the late Holocene warm periods. Several studies pointed out neoglacial advances and retreats in the region during the late Holocene (e.g.: Björck et al., 1991; Hall and Perry, 2004; Abram et al., 2013; Palacios et al., 2020). Ice-free areas on the SSI and AP began deglaciation between 9 and 6 ka before present (John and Sugden, 1971; Barsch and Mäusbacher, 1986; Hall, 2009; Toro et al., 2013; Oliva et al., 2016). Although BP has been mainly ice-free since the last retreat of the glaciers, around 5 to 4 ka ago (Björck et al., 1993, 1996; Toro et al., 2013), glacial readvances have been recognized at about 6, 4 and 1 ka before present (Björck et al., 1991; Palacios et al., 2020). After glacier retreat, periglacial and paraglacial processes play a major role in reshaping ice-free landscapes, as glacial sediments and landforms are rapidly reworked and adjusted to new environmental conditions. In BP, different places on Livingston Island and other ice-free areas within the northern Antarctic Peninsula including the surrounding islands, these processes strongly influence slope stability and sediment transfer toward fluvial and coastal systems (Oliva et al., 2016; Ruiz-Fernandez et al., 2019).

Streams within ice-free areas of maritime Antarctica are influenced by periglacial, glacial and fluvial processes, lithology, topography and meteorological conditions, determining rapid change in the freeze and thaw cycles (Rochera et al., 2010; Pla-Rabes et al., 2013). The ice-free areas of the SSI are snow covered for most of the year, however, by the end of the austral summer, nearly all the snow will have disappeared and where surface and subsurface drainage systems are characteristic features of the ice-free areas (López-Martínez et al., 1996b). Furthermore, the presence of permafrost affects the hydrology of the streams and the active layer, which thaws during the austral summer and contributes to streamflow. As temperatures increase, changes in permafrost can alter water availability and stream dynamics (De Pablo et al., 2023).

The SSI are within the warmest region of Antarctica (King and Turner, 1997; Turner et al., 2004). Since 1950, the AP region has experienced extraordinary rapid warming (Vaughan et al., 2003). The increase in temperature has led to glacier retreat in the region, as indicated by studies showing a 10.0 % ± 4.5 decrease in the ice volume of glaciers on Livingston Island from 1956 to 2000 (Molina et al., 2007).

Although most of the studies highlight a general warming trend in the AP and the SSI, it was observed that a deceleration of the regional warming trend occurred during the 2006–2015 decade in the northern AP region that drives the seasonal changes in the SSI, although with a time delay (Oliva et al., 2017). In the mentioned decade, lower summer temperatures resulted in a longer duration of snow cover in the area and suggest a cooling trend (De Pablo et al., 2017; Ramos et al., 2017). This also means that a regional (winter) cooling in these years involved a slow-down of glacier recession, a shift to surface mass gains of the glaciers (Navarro et al., 2013; Turner et al., 2016; Oliva et al., 2017; Shahateet et al., 2021).

In general, permafrost is absent at low elevations (Vieira et al., 2010; López-Martínez et al., 2012; Bockheim et al., 2013; Ferreira et al., 2017) and glacier retreat in the SSI and AP region has accelerated in response to rising air temperatures, with increases of approximately 0.5 °C per decade (Turner et al., 2004; Steig et al., 2009). This accelerated ice loss has significant implications for the region's landscape and hydrology. Mean annual precipitation in the studied area is relatively high, reaching 500 mm per year, mainly as snow during autumn and winter seasons (Bañón, 2001; Rochera et al., 2010; Bañón et al., 2013). Studies show that the permafrost active layer thickness has increased since the mid-20th century in the SSI (Vieira et al., 2010; Bockheim et al., 2013).

Temperature is a key factor influencing the hydrological regime during the summer season, which controls runoff volumes, but solar position and geomorphic factors also control melt volumes (Conovitz et al., 1998) as well as changes in sea-ice concentration (Zwoliński et al., 2016). Antarctic hydrological systems are paralyzed most of the year as temperatures are below freezing point and only during the short austral summer the water systems are active (Lecomte et al., 2016; Kavan, 2022). Antarctic streams have a hydrological regime highly variable interannually as well as on a daily basis, with little overland flow and the dominance of hyporheic flow path (Gooseff et al., 2003). Conditions nowadays suggest that there is a high chemical weathering of the land surface (Kavan et al., 2017). The geomorphic processes in channels can be very different from the SSI to other regions within Antarctica where the total sediment yield in deglaciated catchments ranges from 68 to 186 t km^{-2} yr^{-1} in the James Ross archipelago (Kavan et al., 2017; Kavan, 2022). This is considerably higher than the specific case of Deception Island with volcanic activity, where Inbar (1995) recorded values of 46 t km^{-2} yr^{-1}. Zwoliński et al. (2016) provides an assessment of denudation rates on King George Island based on suspended and dissolved loads in glacierized and non-glacierized catchments, estimating values ranging from 7.2 to 214.3 t·km^{-2}·d^{-1} and from 0.3 to 72.5 t·km^{-2}·d^{-1}, respectively. These results suggest the significant role of meltwater derived from direct glacier melting in controlling sediment and solute fluxes within the system. Similar studies in King George Island have also documented a large seasonal variability (between 0.2 g m^{-2} d^{-1} in winter and 2.6 g m^{-2} d^{-1} in summer) in sediment fluxes in shallow coastal locations (Khim et al., 2007), Further comparison of sediment yield data is lacking for other areas of the SSI.

The study of river morphology and stream channel characteristics focuses on factors such as equilibrium channel size, pattern, and slope, with key research by Leopold et al. (1964) and Park (1978) highlighting the critical role of water and sediment discharge in shaping these attributes. Streams achieve a steady state when channel capacity grows at the same rate as the drainage area (Park, 1978). Morphometric characteristics such as steady bankfull flow frequency are important for studying rivers (Woldenberg, 1966; Phillips et al., 2022). In our study, bankfull discharge can be used as a mean discharge (Park, 1978), which can be considered useful in ungauged areas such as the SSI.

Glacial retreat and the permafrost and active layer evolution are main drivers of surface and subsurface hydrological processes in ice-free areas of the studied region (Falk et al., 2018). Fluvial streams, exhibit episodic work and extreme variability, with frequent lake outburst floods occurring in areas like BP (López-Martínez et al., 1996b). BP is the ice-free area in the SSI in which the drainage system is more developed, has been most mapped in detail compared to other areas and has been object of more quantitative analysis (Birnie and Gordon, 1980; López-Martínez et al., 1996a, 1996b; Mink et al., 2014). However, studies that relate changes in water supply with fluvial morphological features are scarce in the SSI. The aim of this work is to further contribute to the knowledge of the drainage system evolution and its connection with the glacial retreat on BP by means of: (1) Analyzing morphometrical measurements of the stream channels and the equilibrium state of different channels along three watersheds of BP; (2) identifying factors affecting the channels such as precipitation, seasonal snow patches, freeze/thaw, hyporheic and overland flow, and extraordinary events though the analysis of flow levels; and (3) relate fluvial morphological features with current stream regime and past conditions such as those reflected by misfit channels. The study of the drainage systems provides a valuable means to identify geomorphological evolution and to anticipate the possible consequences of future changes in ice-free areas of the SSI.

2. Study area

BP is located on the western end of Livingston Island in the SSI (Fig. 1). With 60.6 km^2, it is the largest ice-free area in the archipelago and comprises altitudes rising from sea level to a maximum of 265 m above sea level (a.s.l.) (Thomson and López-Martínez, 1996). The peninsula contains 110 lakes and pools large enough to be shown on a map at 1:25,000 scale (López-Martínez et al., 1996a, 1996b) and, due to BP scientific interest and degree of conservation, it was designated as an Antarctic Specially Protected Area (ASPA No. 126) under the Antarctic Treaty System.

BP is within a region that experiences mild winds throughout the year and with moderate liquid precipitation in the summer (Bañón et al.,

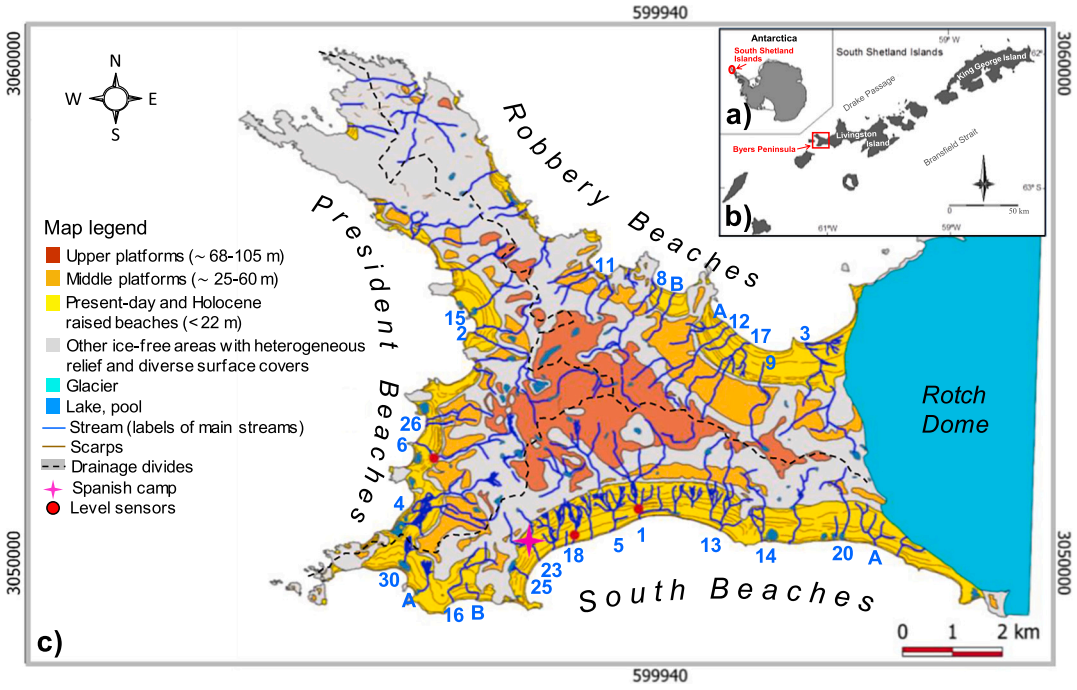

Fig. 1. Study area a) in Antarctica, within the b) South Shetland Islands and c) Byers Peninsula geomorphological map with the streams network studied indicating main drainage divides (López-Martínez et al., 1996a, 1996b) and numbering according to the basin sizes (Mink et al., 2014). The letters indicate additional streams studied in this work.

2013). Low-pressure systems create windy and wet conditions along the coastal regions, contributing to high cyclogenesis (Simmonds et al., 2003; Turner et al., 2004). The relatively flat and undulating topography of the peninsula facilitates the occurrence of stronger winds compared to more topographically protected areas found in the SSI (Ruiz-Fernández and Oliva, 2016). González et al. (2018) notes five atmospheric patterns, where the conditions of low pressure over the Amundsen and Bellingshausen Seas (LAB) produce precipitation and warm conditions in the SSI. Precipitation in the SSI is primarily frontal and in the form of snow, but during the summer, when temperatures often exceed 0 °C, precipitation may occur in liquid form. The mean annual temperature on BP is −2.8 °C, with summer mean temperatures ranging between 1 and 3 °C (Bañón et al., 2013). Daily maxima can reach up to 10 °C, while daily minima may drop to −10 °C. Despite being snow-covered for much of the year, BP becomes mostly snow-free by the end of the summer.

The rocks that outcrop on BP are predominantly Jurassic to Cretaceous volcanoclastic and detrital sedimentary rocks, including Late Cretaceous sills, plugs, and other intrusive bodies (López-Martínez et al., 1996a, 1996c). The present morphology of the peninsula has a series of extensive platforms and much of the coastal area is occupied by present and Holocene raised beaches (López-Martínez et al., 1996a, 1996c). The absence of shrub vegetation in ice-free areas makes the soil surface very sensitive to atmosphere dynamics, especially in the western sector of the AP region where BP is located (De Pablo et al., 2023).

Geomorphological processes in BP include extensive periglacial activity and are very influenced by permafrost dynamics and evolution of the active layer, whose thickness varies from about 30 cm to more than 1 m depth at altitudes above 20 m a.s.l. (Serrano et al., 1996, 2008; Bockheim et al., 2013; Vieira et al., 2010; López-Martínez et al., 2012).

De Pablo et al. (2023) suggest that current climate change is showing impacts on seasonal and perennially frozen soils. There is a significant presence of water in the soil coming from melting snow cover in spring. In this case, the number of days with snow cover for BP increased from 2010 and 2011 (below 300 days) to 2012 and 2015 (340 and 350 days) and then decreased in 2016 and 2018 (below 300 days) (De Pablo et al., 2014). Lateral runoff enters the stream channels through surface and subsurface layers and as soils thaw, subsurface water flow can increase lateral water flow through thawed zones (Woo, 2012). Like on BP and other areas in the SSI, stream flows are conditioned by several factors during summer period, such as snowmelt, rainfall events, surface water evaporation and permafrost melting as well as the influence of marine aerosol deposition (i.e. sodium and chloride) which influences the chemical content of the surface waters due to the close proximity to the coast (Toro et al., 2007).

BP has one of the highest concentrations of stream channels of all the SSI and is the area of the archipelago having more studies focused on fluvial geomorphology. Some of them are related to stream and lake morphologies and basins and streams mapping and ordering (López-Martínez et al., 1996a, 1996b) and others include detailed quantitative analysis of the fluvial system and connect its evolution to the BP deglaciation history (Mink et al., 2014). Regarding water supply, Birnie and Gordon (1980) described seven different relationships between topography and meltwater, and they suggest that channels originated from snow patch drainage systems. Mink et al. (2014) indicates that morphometric parameters reveal the evolution of basins and a limited hierarchical network, common of a youthful stage of landscape evolution models. Using morphometric indexes, Mink et al. (2014) detect changes in water supply during the peninsula's deglaciation process. Overland flow has been reported from snow melt erosion which occurs when a large winter accumulation of snow is subjected to rapid thaw (Birnie and Gordon, 1980) and from direct meltwater from glaciers, mostly Rotch Dome (López-Martínez et al., 1996c).

According to López-Martínez et al. (1996b) there are three main basins, including each one of them a series of sub basins, that drain most of BP: Southern Streams (SS) flowing to the South Beaches (18.9 km^2), Western Streams (WS) flowing to President Beaches (20.3 km^2) and Northern Streams (NS) through the Robbery Beaches (20.3 km^2). Between the south and west coast, there is an area of Southwestern Streams (SWS), which flow into a rocky area and there are certain areas of undefined or endorheic drainage (Fig. 1). BP has a dense drainage network with the longest streams ranging between 2.8 km, 3 km and 4.5 km in the south, north and west sub-basins, respectively (López-Martínez

et al., 1996b). Mink et al. (2014) carried out a morphometric index analysis along 30 individual basins, which include the ones that are analyzed in this paper. The size of the basins varies between 3.23 km^2 (SS-1) to 0.54 km^2 (SS-30) with a mean area of 1.26 km^2. The highest Strahler order is 4, but this is only valid for a few of the basins, and where the order of 3 is dominant (López-Martínez et al., 1996b). The streams dissect the ice-free area and depending on the year, snow and ice patches are often present within the basins. Overland flow is irregular and occurs mainly during the warmer summer season (with temperatures fluctuating around 0 °C). This is strongly linked to changes in air temperature in summer, which produce large fluctuations (López-Martínez et al., 1996c), but precipitation has also been reported as a source of surficial water in channels (Cuchí et al., 2004). Sometimes the flow is generated beneath the snow/ice patch forming tunnels (López-Martínez et al., 1996b). As reported by Birnie and Gordon (1980), the identification of drainage networks is complicated due to the shared snow patch sources, and water divides, which are sometimes diffuse and with areas of undefined drainage (López-Martínez et al., 1996b). Erosion on BP landscape has been linked to meltwater produced by thawing snow (Birnie and Gordon, 1980). As a result, the sources of sediment deposits are both in channels (López-Martínez et al., 1996b) and in lakes (Björck and Zale, 1996). In BP, as occur in other ice-free areas and also referred to as polar oases, frequent morphological changes occur in response to environmental variations ("the cascade system"), such as ground temperatures exceeding 0 °C and the presence of liquid water during the warm period, resulting in irregular hypsometry (Zwoliński et al., 2016).

Common morphotypes along stream channels in BP include diffuse drainage in the uppermost headwater plains, often flowing into lakes in the upper platform. Downstream of these, the network is transformed into braided systems, and when the platforms are eroded, small canyons develop. Finally, on the plains that form the Holocene raised beaches, they are transformed into open braided systems, with wedging in some parts between beaches at different heights and with multichannel or diffuse zones in the flatter areas (Fig. 2).

The landscape with gentle slopes in upper basins characterizes the diffuse drainage systems related to platforms that results in vast flat areas in which channels show limited incision capacity (Fig. 3A). The resultant low energy is unable to erode and incise the channels. On these platforms, snow patches are widely distributed and thaw processes during summer provide a large amount of overland flow, which results in frequent subsurface flow from the active layer-melting zone (López-Martínez et al., 1996b; Mink et al., 2014).

As the upper platform has been affected by glacial processes, the landscape contains numerous over-deepened depressions which result in the existence of approximately 110 lakes on Byers Peninsula (López-Martínez et al., 1996b) (Fig. 3B). During the winter, the surfaces of lakes are frozen. Downstream of the lakes, there are sections of well-developed braided systems where an increase of slope and sediment in channels is related to the increase of discharge (Birnie and Gordon, 1980).

The lower marine platforms are incised by channels and flow is confined into single and entrenched channels forming canyons in which knickpoints occasionally develop, when more resistant lithologies hinder river incision and upstream erosion (Fig. 3C). Frequently, those canyons are covered by snow patches where flow is confined to temporary tunnels as has been observed in Byers Peninsula by López-Martínez et al. (1996b) and in King George Island (Zwoliński, 2007). The maximum size of some observed tunnels is about 2 m high and 4 m wide, thus, during some extraordinary episodes, the water flows through these tunnels. At the upper end of the tunnels, the collapse of snow at the end of the winter season may block the drainage forming a plug like obstruction. As a result, water is retained in upstream lakes, thus increasing their volume. This increase in water volume exerts pressure on the plug until glacial lake outburst events occur (Cuchí et al., 2004; Toro et al., 2007).

Downstream of the canyons, most of the streams flow along raised beach deposits in braided channels (Fig. 3D). In some sectors, the stream flows in a single incised channel connecting beaches at different heights.

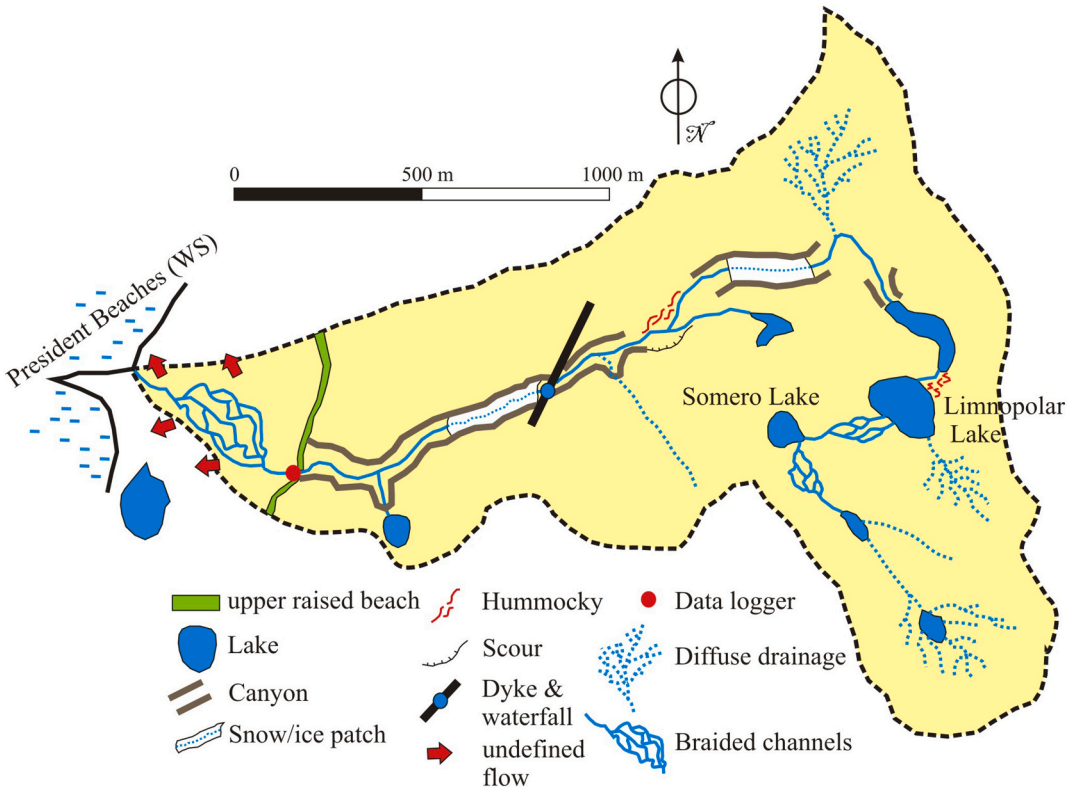

Fig. 2. Simplified geomorphological sketch map of the catchment area showing the diversity of morphotypes along the WS-6 course.

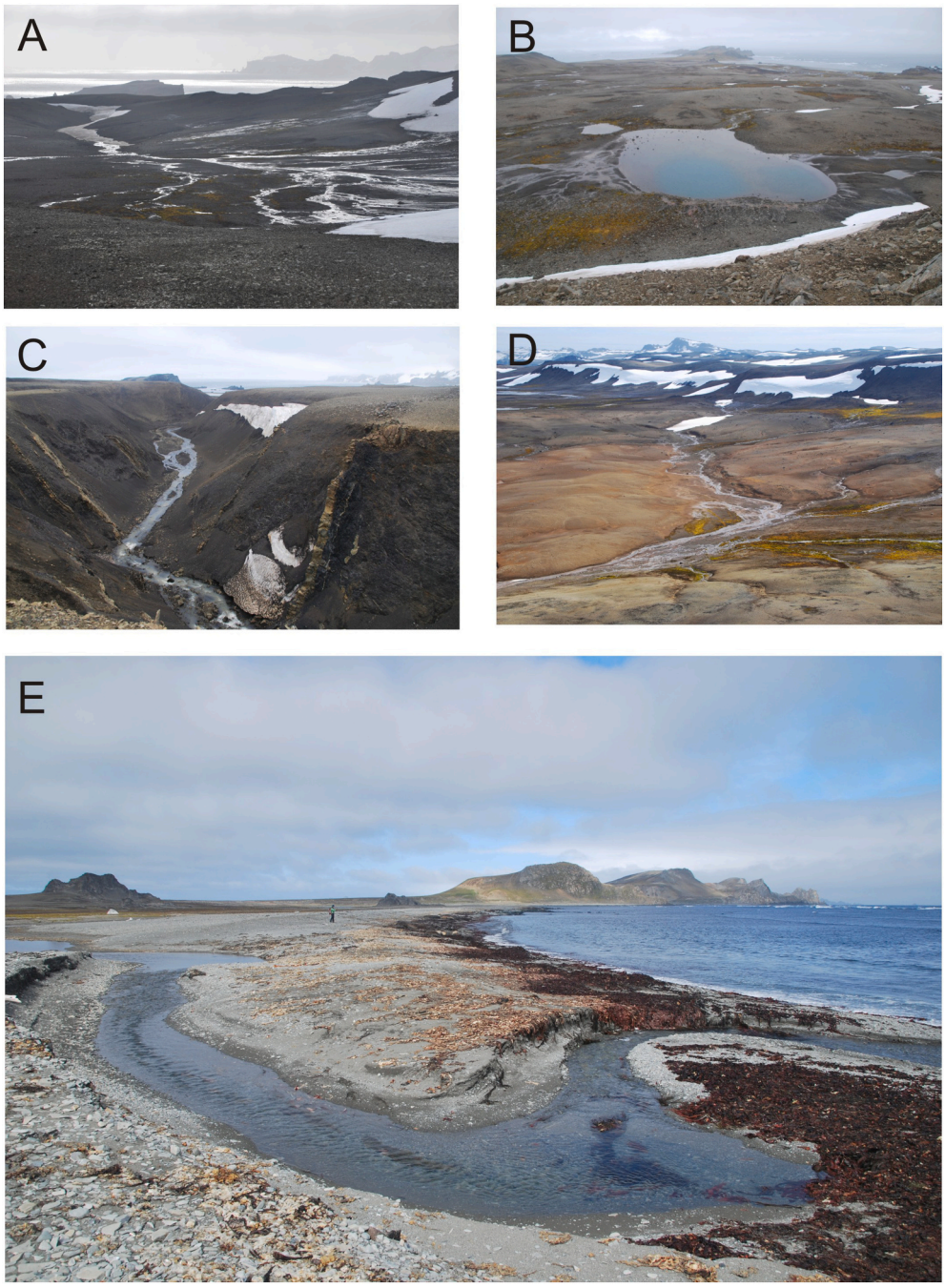

Fig. 3. Morphologies of stream channels. A: Diffuse drainage in upper basins with gentle slope and mostly with hyporheic flow in SS-18, B: Lake collecting diffuse drainage of flat areas in WS-4 basin (approx. 30 m diameter), C: Incised canyons free of ice and snow in WS-6 (approx. 20 m deep), D: Multichannel braided system along intermediate areas, and E: Meandering stream channel in the more recent Holocene raised beaches at the stream mouth in NS-9.

Near to the coast and due to the gentle slope, sediments accumulate and coastal lagoons and submarine small fans are formed (Fig. 3E).

3. Material and methods

3.1. Morphometric measurements

Existing geomorphological maps and previous studies on the BP drainage system and its quantitative analysis (López-Martínez et al., 1996a, 1996b, 1996c; Mink et al., 2014) formed the base to select the streams that were studied in this work. In the present study, morphometric measurements were recorded from 24 January to 6 February 2022 along 26 streams (Table 1) in the main channels in each of the watersheds previously identified and analyzed in BP by the mentioned authors. The streams located in the northwestern sector of the peninsula were not included, as access was prohibited due to the ASPA No. 126 regulations (Antarctic Treaty Secretariat, 2022).

Key morphometric measurements were obtained to determine the degree of stream evolution and equilibrium stage in the fluvial systems and were taken according to standard work carried out on channel processes (e.g. Leopold and Maddock, 1953; Woldenberg, 1966; Park, 1978; Wohl, 2020; Phillips et al., 2022): channel width, depth, slope, size of ordinary channel and major channel. All measurements were determined in the field using a laser rangefinder Trupulse 360R with

Table 1
Locations of morphometric measurements carried out for the stream channels (Northern Streams - NS, Southern Streams - SS, Southwestern streams - SWS and Western Streams - WS).

Stream label	Coordinates (WGS84)		Altitude (m a.s.l.)	Slope (%)	Field observations
	Latitude	Longitude			
NS-3	62°37′48.12″	60°59′23.63″	3	1.1	High discharge from Rotch Dome glacier
NS-8	62°37′4.84″	61°3′16.75″	2	4.7	Wide braided channel, running water, delta
NS-9	62°37′44.18″	61°0′28.91″	1	2.2	Running water, wide channel
NS-11	62°36′58.67″	61°4′25.16″	2	1.3	Running water, catastrophic evidence, canyon upstream
NS-12	62°37′35.76″	61°1′50.28″	2	1.8	Wide channel, snow plug in canyon upstream
NS-17	62°37′42.53″	61°1′21.46″	2	1.6	Low incised, wide outwash
NS-A	62°37′47.15″	61°1′7.96″	2	2.4	Infiltration fan, ephemeral, without direct outflow to the sea
NS-B	62°36′54.34″	61°4′43.68″	2	0.7	Canyon upstream, running water, braided
SS-1	62°39′24.51″	61°3′31.27″	2	2.2	Running water, braided and open channel, meandering downstream, delta
SS-5	62°39′35.66″	61°4′1.54″	1	2.7	Delta, braided
SS-13	62°39′34.78″	61°1′32.46″	3	2.2	Wide braided, entrenched, lagoon
SS-14	62°39′30.74″	61°0′35.32″	8	3.0	Lagoons, ephemeral, outwash
SS-18	62°39′44.55″	61°4′57.75″	1	2.8	Erosion upstream, scour marks, fan, delta
SS-20	62°39′30.53″	60°58′36.98″	8	0.7	Ephemeral, fan and lagoon
SS-23	62°39′50.63″	61°5′26.53″	2	1.4	Braided, lagoon, running water
SS-25	62°39′59.94″	61°5′47.86″	3	2.3	Wide and braided, running water, delta
SS-A	62°39′41.40″	61°4′35.46″	1	4.1	Lagoon, poorly shaped
SWS-16	62°40′23.97″	61°7′51.33″	4	4.1	Ephemeral, wide channel
SWS-30	62°40′16.03″	61°8′43.85″	2	2.8	Ephemeral, open wide channel, lagoon
SWS-A	62°40′25.24″	61°7′8.99″	2	3.6	Fan, lagoon, ephemeral
SWS-B	62°40′34.19″	61°8′26.26″	2	2.6	Ephemeral, incised, lagoon
WS-2	62°37′37.67″	61°7′19.82″	2	1.6	High discharge, wide channel, canyon upstream
WS-4	62°13′34.43″	61°9′33.47″	3	5.1	Running water, wide channel, delta
WS-6	62°38′57.82″	61°8′15.23″	10	1.1	Well shaped, wide braided channel, canyon upstream, delta
WS-15	62°37′21.38″	61°7′20.00″	2	0.4	Low discharge, catastrophic fan, lagoon
WS-26	62°38′32.63″	61°8′16.95″	7	0.5	Catastrophic evidences, fan, canyon upstream, lagoon

±20 cm of accuracy. Basic measurements of major stream parameters were obtained as follows: Bankfull channel capacity (A), bankfull channel width (W), bankfull mean depth (D), width/depth ratio (W/D), wetted perimeter (P), hydraulic radius (R), channel slope (S) and cross section averaged velocity (u) using Strickler's formula (1) and flow discharge (Q). Strickler formula relates water depth and flow velocity of open channel flow based on the assumption of one-dimensional (cross-section-averaged) flow characteristics and was used as a first approximation for boundary conditions.

$$u = k_{st} * S^{\frac{1}{2}} * R_h^{2/3} \quad (1)$$

where: u = is the cross-section-averaged flow velocity in (m s^{-1}), K_{st} is the Strickler coefficient in fictional (m s^{-1}) corresponding to the inverse of Manning's n_m, S = is the hypothetic energy slope (m/m), which can be assumed to correspond to the channel slope for steady, uniform flow conditions and R_h = is the hydraulic radius in (m). A coefficient of Manning's n_m of 0.05, continuous channel and absence of vegetation was considered.

The frequent braided shape of BP stream network makes it difficult to measure a single channel, and thus to obtain inferences on the discharge and bankfull parameters. For that reason, key sections of the streams were selected in those sectors of the Holocene raised beaches where flow is concentrated in a single channel due to the incision where there is a greater slope between the different beaches. It was considered that such sections reflect the erosive power of the stream.

3.2. Discharge measurements

Due to the absence of gauge stations in the area, water and atmospheric pressure sensors containing data loggers (LevelSCOUT 2X and BaroSCOUT 2X) were installed in three sites at selected streams (Fig. 1C). The instruments were located in the lower part of the streams, at their arrival to the Holocene raised beaches having a single incised channel, avoiding sectors with multiple channels and braided morphology frequent on BP. The water level in the stream was obtained from the data loggers subtracting the atmospheric pressure from the water pressure.

Data loggers were installed in two streams for two years, during the period January 2022 to February 2024 as follows: 1) WS-6 at the arrival to the western Holocene raised beaches of this stream that shows the highest degree of morphological evolution (wide canyons and well-defined channels) with a large basin and numerous headwater lakes; and 2) SS-18 at the upper part of the South Beaches, as a sample of small-size basin with a lake in the upper part. A further stream (SS-1) with the largest catchment area of BP was monitored during 14 days of fieldwork

(27 January to 6 February 2022).

4. Results

4.1. Morphometric analysis

Channel size is one of the most important parameters that reflect stream work and relates basin size, discharge and slope as was determined for the different studied streams (Table 1). As established by Wolman and Leopold (1957), A is a proxy for channel size that indicates the importance of each stream.

In the SS (Table 2), SS-5 had the largest channel size (47.4 m^2) but not the largest basin, followed by SS-18 (34.8 m^2) and SS-20 (31.9 m^2). However, SS-1 has the largest basin area (3.23 km^2) although its A measured only 23.4 m^2. In the NS, however, the order is directly related to the size, the largest A was NS-3 (51.4 m^2) and there was a big difference between NS-3 and the other channels. It is important to note that this stream drains the melt waters of the Rotch Dome Glacier. Following the same pattern as the South Beaches, WS do not keep the order. WS-6 had an oversized channel that was larger than its present A (65.3 m^2) and clearly larger than all the other channels. This may indicate a source of misfit stage and changes in stream evolution along with the deglaciation process. SWS are rocky channels, and the size did not reveal differences between them.

W/D is one of the most used parameters of cross-sectional geometry and was used to infer the limit strength and relative erodibility of bed and bank materials as well as relative base level stability (Wohl, 2020). In this case, NS and WS showed similarities in average W/D values around 38–39 (Table 2). Southern channels (W/D = 27) have more entrenched channels and are less wide than the ones from the North and from the West. Measurements were taken in streams located on raised beaches; thus, lithological control is not a distinctive factor here. We believe that S plays an important role in these differences with average values of 0.024 m/m on Southern streams and 0.017–0.019 m/m in NS and WS. Higher slopes provide more energy to the system, channel incision and a reduction of W/D. Another important point is that if discharge increases with time at a cross section, channels become wider more rapidly. This would affect the streams where the glacier limit remains stable for a short time during the deglaciation process, and thereafter the glacier retreats and leaves the channels in a misfit situation. For example, SS-A is located near the southern boundary of Rotch Dome and has a higher width to depth ratio (45.3) despite its small basin size (0.48 km^2). In the NS, the current stream receiving meltwater from Rotch Dome Glacier is NS-3 and its W/D is 35.7. Further misfit channels are NS-17 and NS-A, with high ratios and small basin sizes. Channel widening requires less sediment transport capacity than channel

Table 2
Main morphometric measurements of streams on raised beaches. AA: bankfull area, W: bankfull width, D: bankfull mean depth, W/D: width/depth ratio, P: wetted perimeter, R: hydraulic radius, S: channel slope, u: cross section averaged velocity and Q: discharge (location of streams are in Fig. 1).

Stream number	A (m^2)	W (m)	D (m)	W/D	P (m)	R (m)	S (m/m)	u ($m \cdot s^{-1}$)	Q ($m^3 \cdot s^{-1}$)	Basin area (km^2)[1]
Southern Streams (SS)										
SS-1 (dl)[2]	23.4	29.2	0.8	36.5	30.8	0.8	0.022	2.5	58.5	3.23
SS-5	47.4	39.5	1.2	32.9	41.9	1.1	0.027	3.6	170.6	1.91
SS-13	28.1	23.4	1.2	19.5	25.8	1.1	0.022	3.1	87.1	**0.7**
SS-14	25.5	14.2	1.8	7.9	17.8	1.4	0.030	4.4	112.2	1.08
SS-18 (dl)	34.8	29	1.2	24.2	31.4	1.1	0.028	3.6	125.3	0.98
SS-20	31.9	22.8	1.4	16.3	25.6	1.2	0.007	1.9	60.6	0.73
SS-23	24.2	30.2	0.8	37.8	31.8	0.8	0.014	2	48.4	0.7
SS-25	3.6	9	0.4	22.5	9.8	0.4	0.023	1.6	5.8	0.62
SS-A	29	36.2	0.8	45.3	37.8	0.8	0.041	3.4	98.6	**0.48**
Average	**27.5**	**25.9**	**1.1**	**27**	**28.1**	**1**	**0.024**	**2.9**	**85.2**	**1.15**
Northern Streams (NS)										
NS-3	51.4	42.8	1.2	35.7	45.2	1.1	0.011	2.3	117.2 (*)	2.53
NS-8	7.8	9.8	0.8	12.3	11.4	0.7	0.047	3.4	26.6	1.65
NS-9	19.1	31.8	0.6	53	33	0.6	0.022	2.1	39.4	1.59
NS-11	11	11	1	11	13	0.8	0.013	2	22.5	1.4
NS-12	7.7	12.8	0.6	21.3	14	0.5	0.018	1.8	13.9	1.39
NS-17	13.5	33.8	0.4	84.5	34.6	0.4	0.016	1.4	18.4	1.04
NS-A	11.8	29.4	0.4	73.5	30.2	0.4	0.024	1.7	19.6	**0.39**
NS-B	8.5	10.6	0.8	13.3	12.2	0.7	0.007	1.3	11.2	**0.41**
Average	**16.3**	**22.8**	**0.7**	**38.1**	**24.2**	**0.7**	**0.019**	**2**	**33.8**	**1.3**
									21.7 (**)	
Western Streams (WS)										
WS-2	12	15	0.8	18.8	16.6	0.6	0.041	2	24	2.67
WS-4	10.1	16.8	0.6	28	18	0.6	0.051	3.1	31.3	2.28
WS-6 (dl)	65.3	40.8	1.6	25.5	44	1.5	0.011	2.7	176.3 (*)	1.9
WS-15	21.9	27.4	0.8	34.3	29	0.8	0.004	1.1	24.1	1.08
WS-26	14.3	35.8	0.4	89.5	36.6	0.4	0.005	0.8	11.4	0.6
Average	**24.7**	**27.2**	**0.8**	**39.2**	**28.8**	**0.8**	**0.017**	**1.9**	**66.4**	**1.7**
									22.7 (**)	
Southwestern Streams (SWS)										
SWS-16	13.3	18.8	2.4	31.3	20	0.6	0.041	2.8	37.2	1.06
SWS-30	11.6	29.2	1.8	73	30	0.4	0.028	1.8	20.9	0.54
SWS-A	5.1	12.8	2	32	13.6	0.4	0.036	2	10.2	**0.18**
SWS-B	4.1	20.4	1.8	102	20.8	0.2	0.026	1.1	4.5	**0.37**
Average	**8**	**20.3**	**2**	**59.6**	**21.1**	**0.4**	**0.033**	**1.9**	**18.2**	**0.5**

Note: ([1]) Areas marked in regular text according to Mink et al. (2014) and areas in bold text estimated from the field measurements, (*) discharge outliers, (**) average excluding discharge outliers, (dl): sections with level sensor containing data logger.

deepening (Wohl, 2020) and the difference in channel slope between SS and others may be the reason for the different patterns. There is geomorphological evidence for this process. SS end in submerged fans, a product of sediment transport. In contrast, the Western and Northern coast had fewer coastal fans. Bank erosion in the widening process implies resulting sediment stored in the channels, whereas bed erosion requires sediment entrainment and downstream transport (to the coast, forming fans). Low bank erodibility reflects bedrock in the bank as the SWS reflect in their W/D of 59.6.

Other morphometric measurements that support the results are P and R. P is the part of the channel that is in contact with water and represents the friction that slows the velocity of the river. The longer the P, the more friction between channel and water and hence less energy available for sediment transport. Higher values of P were determined for NS-3 (45.2), SS-5 (41.9) and WS-6 (44). NS have smaller average *P* values compared to the SS and WS. R is a measure of the efficiency of a stream channel. It was calculated by comparing P with the cross-sectional area of the channel. The higher the R, the more efficient the stream. Average values of R show more efficiency in southern streams (R = 1) compared to NS and WS (0.7 and 0.8, respectively), however, large streams such as NS-3 (1.1) and WS-6 (1.5) show similar values to the southern ones. This can be a proxy for evolved channels. Again, it is significant that lager basin in size (SS-1) has less efficiency (*R* = 0.8), less morphological capacity (A = 23.4), high W/D ratio (36.5) and less slope (S = 0.022 m/m) than other channels located on the southern coast.

The morphological characteristics for the different streams show clear general trends (Fig. 4 and Fig. 5) except for a few outliers (WS-6, WS-4, WS-2, NS-3, SS-1, SS-5). We hypothesize more about the reasons for this behavior in the following sections related to stream discharge and the occurrence of extraordinary events.

4.2. Discharge estimation from morphometric measurements

The bankfull discharge values represented by the A indicate wider channels and higher capacity in the streams of the southern basins. The estimated discharge using A and Strickler's formula for velocity gives an average of 85.2 $m^3 s^{-1}$, but there is dispersion in data, with maximum values of 170 $m^3 s^{-1}$ and lower values of 5.8 $m^3 s^{-1}$. In this case, a higher bankfull discharge does not correlate with higher drainage areas. Some outliers are present in each basin, especially SS-18, the fifth basin in size, but the second in theoretical bankfull discharge. We interpret this because of erosion in extraordinary glacial outbursts. However, other channels such as SS-A shows high bankfull capacity although it is a small basin area as well as in dry conditions during the field campaign. This will imply a misfit stage due to quick glacier retreat with a "freeze" of former conditions. Present geomorphic work is unable to evolve those channels to the equilibrium size.

NS show bankfull average values around 33.8 $m^3 s^{-1}$ (21.7 $m^3 s^{-1}$ if we exclude the outlier), however stream NS-3 has a higher value of 117.2 $m^3 s^{-1}$. This stream is one of the main drainage ways of the Rotch Dome Glacier meltwaters and is within the third largest basin. The rest of basins in the northern area present similar bankfull discharge values. No extraordinary events were identified in this area.

In the WS, similar results were obtained to those in the northern basin. With an average of 66.4 $m^3 s^{-1}$, (22.7 $m^3 s^{-1}$ if we exclude the outlier). The largest bankfull discharge corresponds to WS-6 stream, the third in basin size in the area, but clearly the largest in bankfull discharge with 176.3 $m^3 s^{-1}$. By means of field analysis, high water marks (HWM) of extreme flood events due to glacial lake outburst were determined. It is significant that basins such as WS-2, the second in size of all BP, have channel dimensions and bankfull discharge of 24 $m^3 s^{-1}$, which is similar to WS-4. We believe this may imply a high degree of channel evolution and a drainage network adapted to present conditions. Those channels show the highest Strahler order of BP and the lowest values of hypsometric integral that could represent a more mature stage (Mink et al., 2014).

The SWS are small size rocky channels with an average discharge of 18.2 $m^3 s^{-1}$. Those values are well adapted to present overland flow as the basin areas are small with an average size of 0.5 m^2.

Plotting bankfull discharge against drainage area (Fig. 4), we found a good level of fit in less evolved basins: SWS rocky area with $R^2 = 0.8$ and NS streams with $R^2 = 0.60$, excluding NS-3 stream). Other basins show low R^2 adjustment (Southern and Western channels with 0.06 and 0.05 respectively). However, if we exclude outliers (SS-1 and WS-6), R^2 adjustment results in SS = 0.6 and WS = 0.7.

We interpret that basins on BP are adequately adjusted with a range of R^2 = 0.6 to 0.8. Extraordinary events can modify main channel characteristics, being oversized in relation to the size of the watershed. This implies that bankfull channel dimensions have some ability to make predictions, however some channels are still in a misfit evolutionary level.

A similar result comes from the plot of A and basin area (Fig. 5). Results were grouped in clusters with certain outliers, which also correspond to the streams with lower numbers, indicating that they are

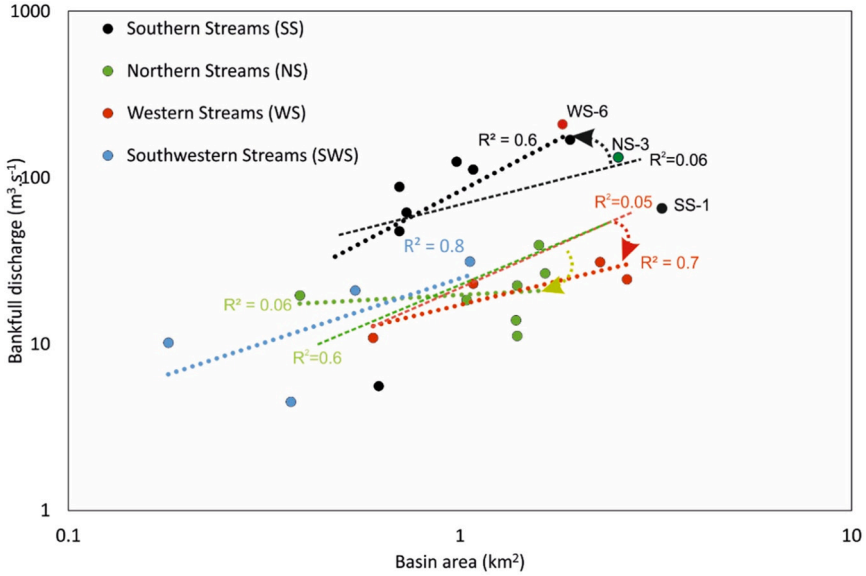

Fig. 4. Different activity (bankfull discharge vs basin area) of channels in the studied basins with and without outliers (WS-6, NS-3 and SS-1).

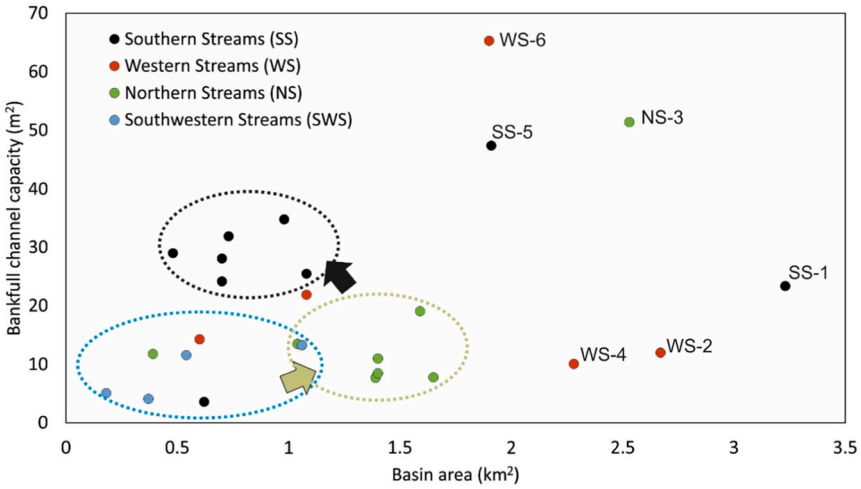

Fig. 5. Comparison between basin area of the drainage system and their A. Circles show general clusters whereas isolated dots reflect outliers and the number of the stream.

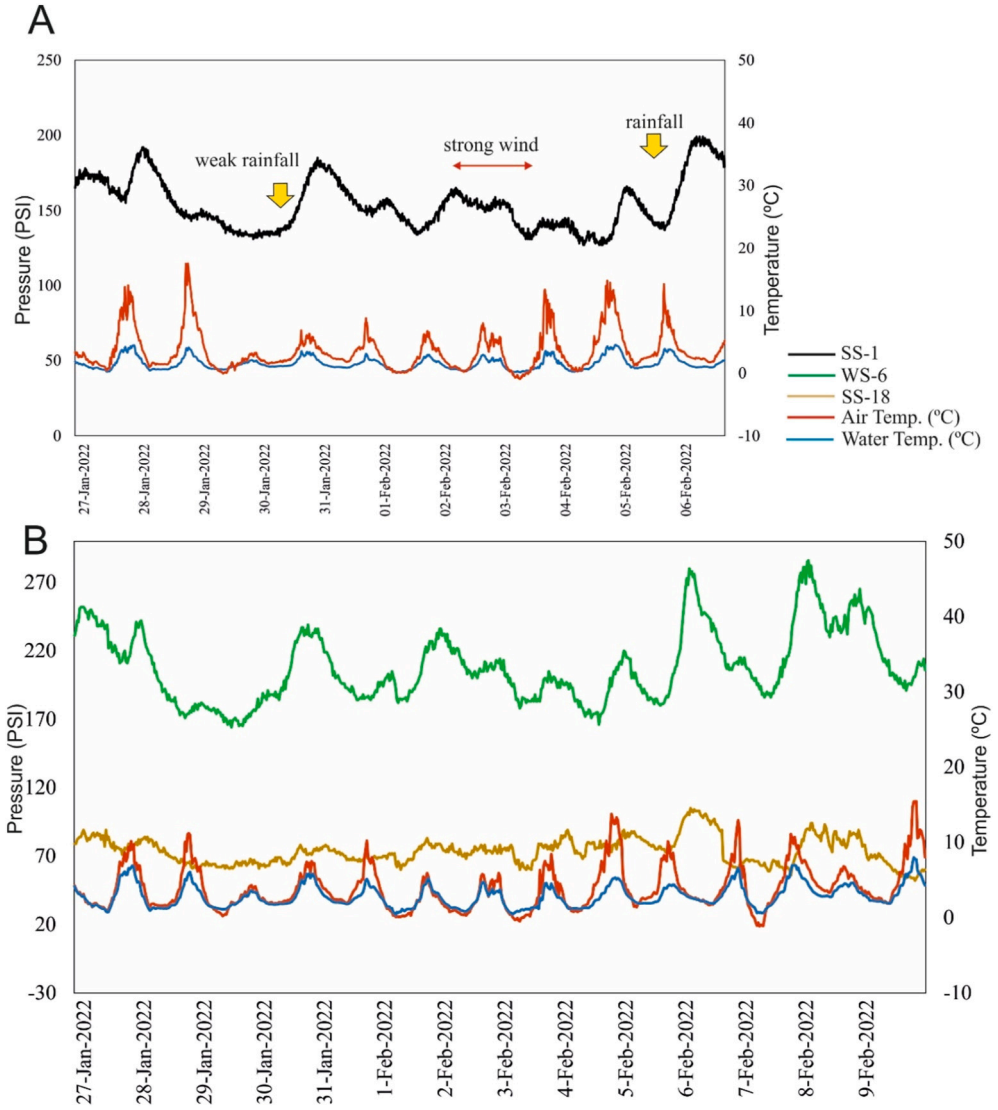

Fig. 6. Overland flow levels in SS-1 (A) and in WS-6 and SS-18 (B) in January–February 2022.

channels with larger basins (the rivers in the area have been numbered according to basin size; see Mink et al., 2014). SWS streams are the least evolved, with similar size of channels despite their basin size. This is common in bedrock channels that require more time to adjust their dimensions due to the hard nature of the channels. NS are also grouped (except for NS-3) and show similar results: larger basins, but similar A. Most of the NS have more ability to erode and resize their channels and watershed.

Regarding the SS, they are bigger in A, which implies there are more erosional processes involved although the basins are not larger. This could indicate an increase in channel slopes and in incision capacity. However, not all the channels fit well with the cluster. There is a group of streams growing in size; both in A and watershed, and this could be a sign of drainage evolution.

WS are not grouped within a cluster. Larger streams are located as outliers, and a few basins keep their small dimensions. However, we detect differences among them. While WS-2 and WS-4 shows the increase of basin area and channel size, probably due to drainage evolution, WS-6 exhibits a larger channel dimension, which is out of line with the size of the watershed. We interpret these as extraordinary events by glacial lake outburst, widely mentioned in this paper.

However, another possible interpretation is that in streams with

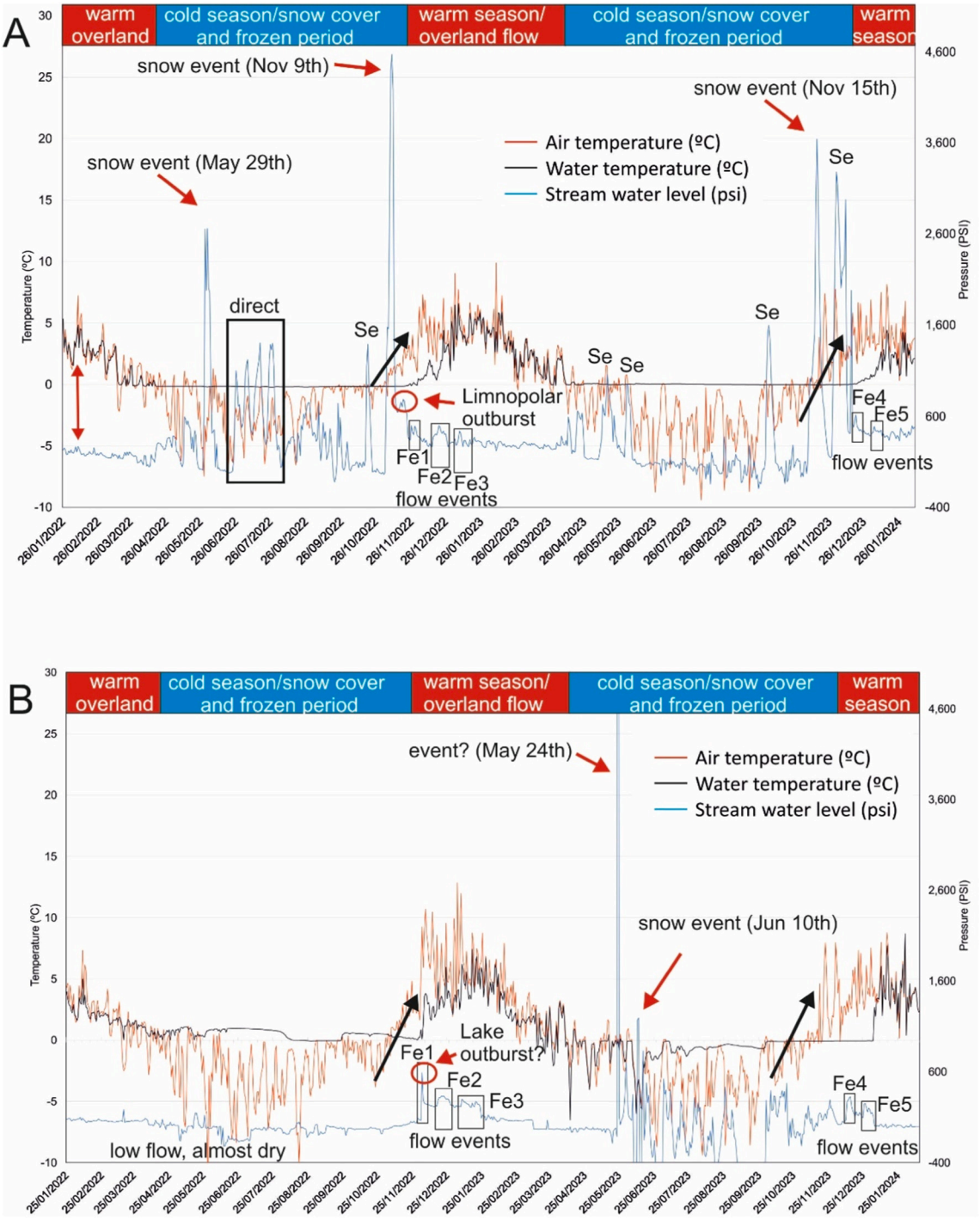

Fig. 7. Water levels in the channels from 20/1/2022 to 25/01/2024 recorded with dataloggers. A: Stream WS-6 on the Western coast. B: Stream SS-18 on the Southern coast. The black arrows show an increase of temperatures resulting in flow events.

large, well-developed basins, the bankfull channel capacity has evolved in response to the magnitude and frequency of discharges. These are sometimes very high due to glacier melting contributions (NS-3), in other cases due to extraordinary events (WS-6), while others reflect past conditions, with large basins receiving relatively low water input (e.g., WS-4).

4.3. Water level estimation from pressure sensors

Recorded data were downloaded from the data loggers after 11 and 14 days for the three sites (WS-6, SS-18, and SS-1) during the period of 27-01-2022 to 06 and 09-02-2022 (Fig. 6). Thereafter, the recorded data after two full years were downloaded from the two sites (WS-6 and SS-18) in February 2024 (Fig. 7).

The first set of data collected for 11–14 days (Fig. 6) shows intermittent water levels during continuous overland flow for SS-1, SS-18 and WS-6. These peaks are related to increases in direct precipitation on the basin. However, the role of stream water level as a response to increasing temperature is not so evident. As shown in the figure, the highest temperature peak did not result in a rise in water level at SS-1, as this stream is not glacier-fed. The data were recorded during the warmest part of the season where the water level did not exceed 200 PSI in SS-1 and 280 PSI in WS-6, while the small catchment SS-18 reflects less water level of up to 100 PSI. In-situ observations suggest that levels were subject to very little variation unless exceptional precipitation values were recorded. SS-1 and WS-6 shows similar response to rainfall. The SS-18 shows a much weaker response, only similar in the case of slightly heavier rainfall.

The second data set (Fig. 7) shows two seasons in terms of air and water temperature and its influence on liquid water available for overland flow (above and below 0 °C). However, field measurements show records of running water temperature at one tenth below zero without freezing. These periods correspond well with the ones suggested by Baroni et al. (2005) in Victoria Land. The cold season begins around the end of April and ends in late November to early December. This is clearly indicated by low water temperatures (~0 °C) that suggest frozen streams, but also by an increase in air temperature. The warm season starts in late November to early December and ends in late April, with water temperatures above 0 °C. However, during the transition between the cold and warm seasons, data suggest an intermittent alternation of frozen and thawed days.

Pressure level record shows several peaks at WS-6 and SS-18 (Fig. 7), which do not represent necessarily floods in the channels. Some of the peaks were recorded during the cold season when water and air temperature were constantly below 0 °C, thus overland flow was not probable. These peaks were interpreted as an increase of snow accumulation in the channels (see Fig. 7, snow events indicated as Se), and coincide with increases in temperature due to snowfall, as reported by Bañón et al. (2013) at the Spanish Antarctic Station Juan Carlos I located ~30 km east of BP. Furthermore, Se peaks can be anomalously high due to the effect of freezing ice crystals affecting the pressure sensor, sometimes even showing negative pressure values. Other peaks, with comparatively lower PSI values than the previous ones, were recorded during warm periods with water temperatures over 0 °C. In this case, the peaks were identified as floods in the channels, and their values imply increases in level pressure of the channels up to 800 PSI (see Fig. 7 A and B, flood events (Fe) of Fe1 to Fe5).

Records were similar in the two channels monitored: The blue line (water level in both channels) at WS-6 (Fig. 7A) indicated overland flow (26-01-2022 to 15-04-2022, 20-11-2022 to 09-04-2023 and 19-12-2023 to 08-02-2024). After this period, intermittent flow may occur, associated with occasional increases in air and water temperatures before entering in the colder period. During the cold season, data loggers recorded the first peak on level pressure (2800 PSI) on 29 May 2022. After that, a series of cyclical abrupt changes in surface temperature, leading to changes in pressure level peaks during the cold season (June and July). This was probably related to snowpack accumulation in the WS-6 channel (see Fig. 7a). This sensor is located at the mouth of a narrow channel, where snowstorms may leave significant snow thickness. During the period from August to the end of October, there seems to be no overland flow and only isolated peaks related to sudden increases in temperature above 0 °C (event of 21 October 2022) exist. There was the highest peak flow of 9 November 2022, which marks the end of the colder season. This peak was associated with an increase in surface temperature from 0 to 10 °C (see black arrow) despite water temperature being around 0 °C and was probably related to a snow period (level pressure record 4500 PSI). Camera records from the Limnopolar Lake in the upper basin of WS-6 indicated a glacial lake outburst of 20 of November 2022. This event (Fe1) was also recorded by the datalogger (at 816 PSI). We interpreted the previous event of 9 November as an event of snow with high rates of accumulation in the channels. However, this may also be related to a glacial lake outburst downstream of Limnopolar Lake.

After both events, the warm season showed overland flow in WS-6 with changes in the water level due to permafrost and snow patches melting. Average values of pressure levels were 300 PSI with isolated flood peaks of 500–600 PSI (Fe2 and Fe3). The behavior was very similar during the following season in 2023, with Se events leaving the highest pressure peaks at the end of cold season, and flood events (Fe4 and Fe5) around 400–500 PSI.

The situation in SS-18 (Fig. 7B) was quite similar regarding the air temperature and the water temperature, which was slightly higher. It is important to note that the level sensor does not register the same high pressure peaks during the cold season. This is because the orientation of SS-18 is different, facing south, and topographically it is impossible to accumulate large thicknesses of snow, as the sensor was located on the raised beach, a very flat and windy area, which prevented snow accumulating. Thus, peaks in level pressure were similar in magnitude to flood events in WS-6, around 400–500 PSI, and were recorded during the same date. During the entire recording time, there exists only one very high record in the level pressure sensor (24 May 2023, 18,670 PSI), and we interpret this as an isolated error in the logger or the effect the freezing water over the sensor. This anomalous period correlates before and after with water temperature oscillating between 0 and well below 0, indicating a probable exposure of the sensor out of the stream water. The first analyzed period, from 25-01-2022 to 25-11-2022 shows low flow activity, with the SS-18 channel almost dry and small variations in level pressure. During the warm season of 3-12-2022 to 11-04-2023, a peak in the channel related to an increase of air temperature (see black arrow in Fig. 7B) was detected, which may be due to a glacial outburst (Fe1) and a series of flood events (Fe2 and Fe3) at about 300 PSI. In the second warm season recorded (15-12-2023 to 11-02-2024), we also detected similar trends, with flooding events following an important increase in air and water temperatures (Fe4 and Fe5).

4.4. Extraordinary events

Evidence of extraordinary events related to lake collapse draining large water volumes and forming deep gullies have been quoted in James Ross Island (Sone et al., 2007), and also mentioned for BP (López-Martínez et al., 1996b; Cuchí et al., 2004; Toro et al. (2007). During our fieldwork, we found evidence of extraordinary events in the study area (Fig. 8). The most common are scours on channels, sometimes with large dimensions, as the ones showed in Fig. 8C from the SS-18. This stream is one of the sites gauged with a pressure sensor, where the exceptional peak flow of 3 December 2024 (the photo was taken in 2022, before the sensor recorded data). This would imply a recurrent lake outburst due to the snow collapse at the beginning of the summer season. In the same basin, we identified other evidence such as palaeolevel lines in lakes (Fig. 8C). Those HWM suggest larger water volumes in the lake, because of their height (+3.5 m the highest).

In the WS-6 basin, it is where more evidence of extraordinary events

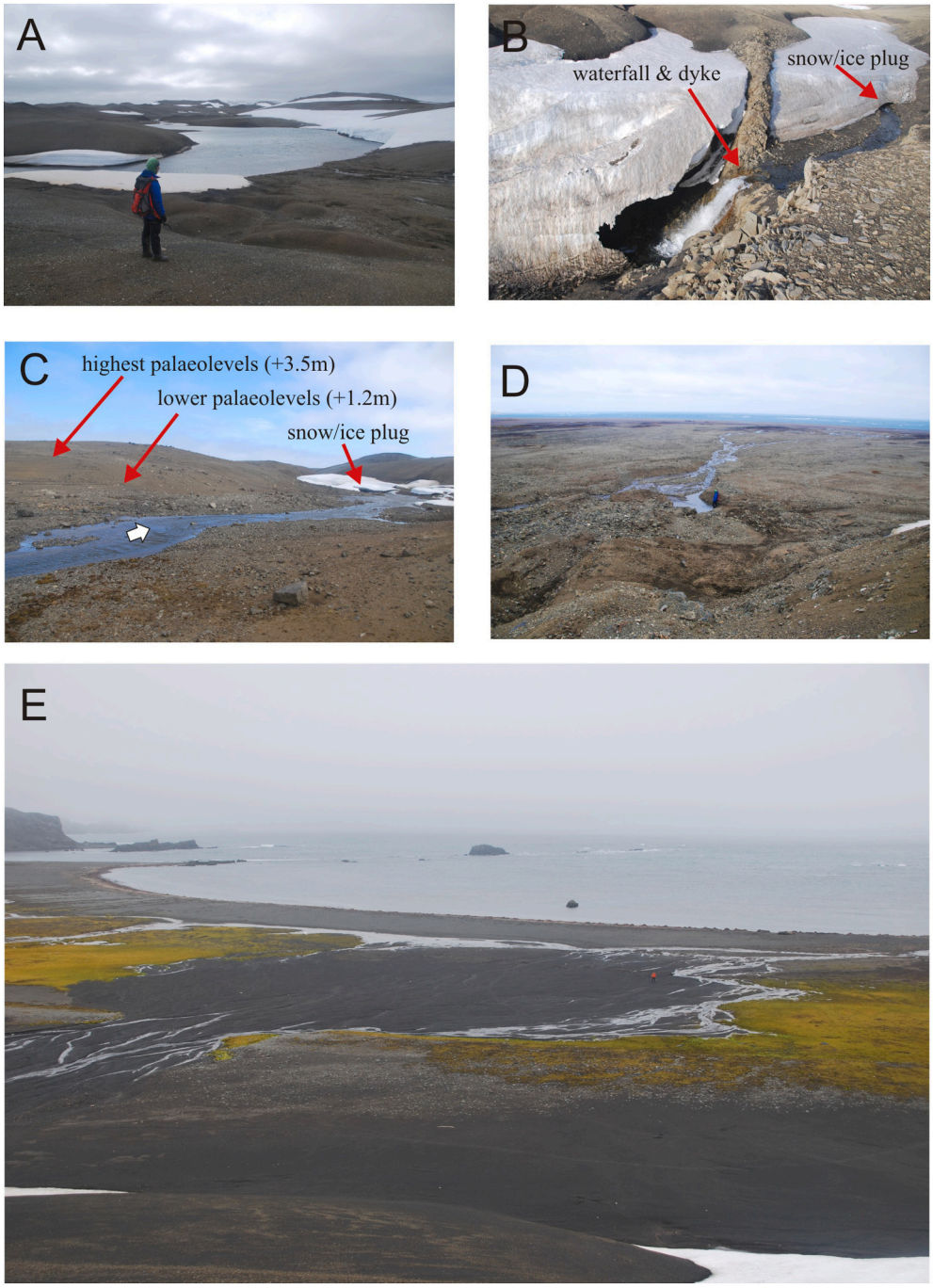

Fig. 8. Evidence of glacial lake outburst in BP. A: Lake in WS-6 basin with hummocky surface from lake collapse, B: Snow-ice patch at the covering the canyons and waterfall controlled by a dyke in WS-6, C: Palaeolevel lines of lake in SS-18, D: Scours from glacial lake outburst in SS-18, E: Fan in WS-15 due to glacial lake collapse that partially covered mosses and former coastal lagoon.

was found. Extensive areas with hummocky relief and downstream canyons were identified (Figs. 8A and 9). These features are a result of the release of large quantities of water that flows at high velocity along the canyons and incised channels that erode the ground in open areas. Along WS-6, at least two areas with hummocky features were identified. At the time of the fieldwork, the two main canyons were covered by snow forming tunnels (Fig. 8B) with smaller dimensions than A on raised beaches incised sites. Peak flow necessarily must be confined and with high speed and erosional capacity. The lower canyon (Fig. 3C) has a wide dimension (40 m wide and 20 m high) that suggests one of the most mature morphologies on BP. Field observations from 2018 to 2024 in the same place show the absence of the snow patch within the lower canyon, demonstrating the temporary character of snow obstructions in the canyon.

Data from the sensors showed (Fig. 7A) some extraordinary events which were recorded with large increases of the peaks on the 9th of November (possible snowfall) and the outburst of Limnopolar Lake on the 20th of November, both related to the first increase of air temperature and the beginning of the summer season. The latter event was recorded by fixed cameras (De Pablo, comm. pers.). A previous event of a sudden decrease in lake level was also recorded in lake Turbio (headwater of SS-18) on the night of the 18th of December 2001 (Toro et al., 2007) and another event in 2002 in some undetermined tributary of the south coast (Cuchí et al., 2004).

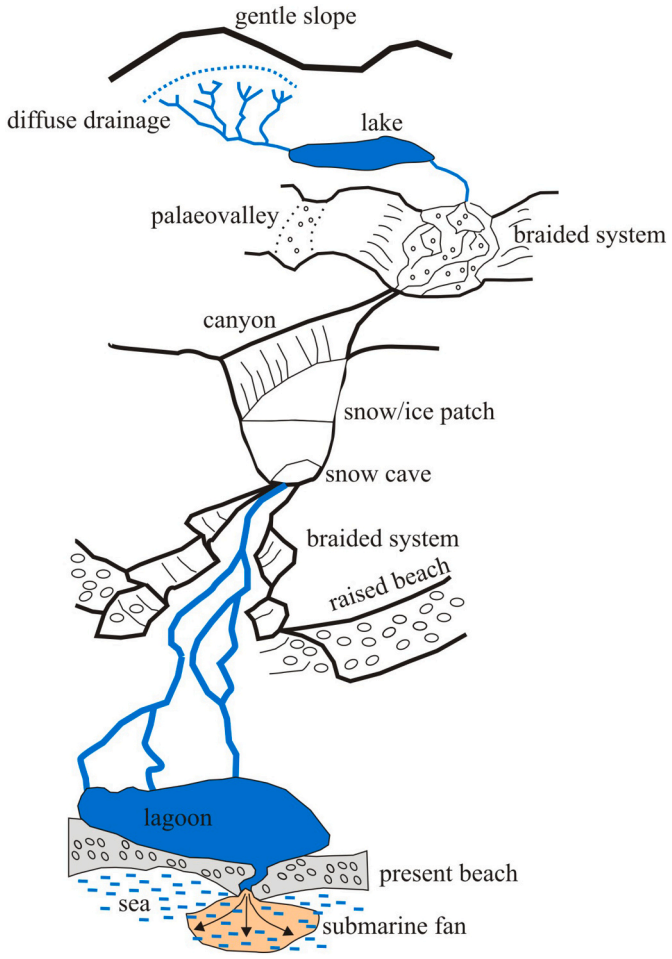

Fig. 9. Scheme of common geomorphological features within a typical catchment basin of a stream in Byers Peninsula.

Further evidence of extraordinary events identified on BP streams are: (1) fan deposition on plains observed in WS-15 (Fig. 8E) and in NS-11, which resulted in a damaged moss cover and the coastal lagoon being buried. (2) sediment washout, except big boulders, along various channels (WS-6, SS-18) which is a product of rapid erosion and high rates of sediment removal, all of them in sites immediately downstream of the lakes, and (3) debris flow in NS-11 that drains larger lakes on BP and make that a large volume of water reached a moraine near Chester Cone and reworks the boulders, generating a debris flow following the emptying of the lake.

5. Discussion

Due to the relief, BP streams tend to be very similar in terms of diversity of morphotypes along their course. This results in the following features along stream channels in BP (Fig. 9): (1) diffuse drainage, (2) lakes in upper platform, (3) braided systems downstream lakes and temporary snow patches, (4) canyons (gullies) cutting raised platforms, (5) open braided systems on raised beaches, (6) entrenched sections on raised beaches slopes, and (7) lagoon and small submarine fan. These observations coincide with those reported by Birnie and Gordon (1980) and López-Martínez et al. (1996a, 1996b). Within this context, morphometric measurements were of great help to understand the erosion and evolutionary processes followed by the streams in the most recent stage. For this study, we focus exclusively on the morphotypes most directly linked to the fluvial environment. Other features such as lakes, deltas, and lagoons were not examined here, although they play important roles in system dynamics and may provide valuable sedimentary records for future work.

Bankfull channel geometry is linked to a characteristic discharge (Leopold et al., 1964) and bankfull flow frequency can be used as a proxy for mean discharge (Park, 1978), which is very useful in ungauged streams such as on BP. Therefore, hydraulic geometry scaling and geomorphic work are important tools to understand stream characteristics in ice-free areas where factors such as vegetation do not play the usual critical role as in warm regions and raised beaches lithology and bed resistance is similar. A acts as a good indicator of the importance of each stream. The raised beaches along the entire lower part of the catchment areas allowed us to interpret channel characteristics and their discharge bankfull capacity. In this case, the A shows the (actual or past) effective work of streams on BP, where the current glacial stage helps to develop wider and deeper channels. Differences in S explain the observed patterns: SS streams end in submerged fans due to sediment transport, while the WS and NS streams have fewer coastal fans (as mapped by López-Martínez et al., 1996a). Bank erosion stores sediment in the channels, whereas bed erosion transports it downstream to form fans. This aligns with Wohl (2020), who states that channel widening requires less sediment transport capacity than deepening. SS streams generally show higher hydraulic efficiency ($R = 1$) than NS and WS streams (0.7–0.8), though large streams like NS-3 (1.1) and WS-6 (1.5) have similar efficiency. NS streams have lower wetted perimeter (P) values on average, while larger basins, such as SS-1, exhibit lower efficiency, reduced morphological capacity, a high width-to-depth ratio, and a gentler slope.

Stream order is linked to stream discharge (Wohl, 2020). The maximum stream order in BP is 4 and only in few more evolved streams (e.g. NS-3). This stream is the current drainage of Rotch Dome Glacier. Other streams acquire their order 4 at the end, near the coast and are related to merged channels in former beach plains (SS-1, WS-4 and WS-7). The low order in most of the rivers (3 or less) shows the limited water supply on channels, except the continuous melt-flow from the glacier. Other channels need an increase in temperature and/or precipitation to have effective discharge. This is well connected with the low sediment supply in the channels mentioned in different Antarctic streams under diverse climatic conditions (Inbar, 1995; Kavan et al., 2017; Kavan, 2022) in comparison to channels in lower latitudes, where the duration of streamflow activity is typically longer. Low rates of sediment supply were interpreted as one of the reasons for channel morphologies with high values of width to depth ratio, as Wohl (2020) suggested. However, changes in sediment yield could have occurred due to the deglaciation process. The main factors that lead to an increase in sediment yield are related to the decrease in snowpack, as De Pablo et al. (2023) pointed out on BP in recent years, the increase in the amount of precipitation, and the increase of glacier meltwaters. Those factors may result in an increase of overland flow with streams fed primarily by glacial melt, with a reduced snow cover. Those streams are expected to experience an increase in sediment load. This response is consistent with global observations showing warming-driven increases in fluvial erosion, sediment transport and delta progradation in cold-region basins (Bendixen et al., 2017; Li et al., 2021). This suggests a trend toward a higher width-to-depth ratio (W/d), distinguishing them from streams that underwent early deglaciation, such as those in the W, SW, and NW regions, consistent with the sequence proposed by Mink et al. (2014), and Oliva et al. (2016). A representative example of this process is the NS-3 system. The most likely circumstances for snowmelt erosion to occur are where a large winter accumulation of snow is subjected to rapid thaw (Birnie and Gordon, 1980), as was recorded with the level sensors (Fig. 7).

During the two seasonal hydrological regimes that were recorded with the sensors, a cold season (April–November/December) with frozen or intermittent flow conditions and a warm season (November–April) with continuous overland flow were clearly identified. The transition periods between these seasons showed alternating frozen and

thawed days, suggesting complex interactions between temperature fluctuations and hydrological response. These results from BP show overland flow during at least 17–21 weeks during the austral summer season. This is more than double of what Conovitz et al. (1998) found in Victoria Land and Kavan et al. (2017) on James Ross Island, where both showed overland flow during six to eight weeks. Such differences reflect the contrasting climatic conditions existing in these geographically distant Antarctic regions. In a qualitative way, Birnie and Gordon (1980) indicate that on BP the melting of snow and fusion of the ice from the glacier dome in early mid-summer leads to an additional water supply, increasing the normal water volume flowing during the rest of the year. The release of these water flows mentioned by Oliva et al. (2017) also increases the available energy of fluvial processes that cause altering actions on the drainage channels during a few months of a year. This continuous measurement of stream functioning will allow, as mentioned by Phillips et al. (2022), to assess the sensitivity of alluvial river geometry to climate change.

Despite the cooling that occurred a decade ago on BP (De Pablo et al., 2017; Oliva et al., 2017), the observed increase of overland flow is likely driven by a warming trend in the AP and SSI (Turner et al., 2004; Rau and Braun, 2002; Kejna, 2003) supporting a net increase in temperature over the long term. Moreover, Quintana and Carrasco (2000) and King and Turner (1997) detected slight increasing trends in precipitation, with a greater number of days of liquid precipitation during the summer and slight decrease in days with dry snow during the winter. The increase of warm and moisture conditions comes from LAB synoptic situation (González et al., 2018). Overland flow correlates strongly with increases in air temperature, while stream freezing occurs when air and water temperatures are around 0 °C. The functioning of streams beneath snow patches was observed while both surface and water temperatures exceeded 0 °C, occasionally with water temperatures below 0 °C. Our findings fit well with recent research from De Pablo et al. (2023) that indicated the number of days with snow cover in general decreased from 2014 to present on BP, Hurd Peninsula (both in Livingston Island) and Deception Island. We believe that the rocky nature of Byers landscape together with a general dark color may increase the surficial temperature in ice and snow free areas and hence, the increase of snowmelt and the frozen soils, the source of hyporheic flow on the channels.

High pressure peaks recorded during the cold season do not always indicate flooding but can be attributed to snow accumulation within the stream channels (Fig. 7), particularly in WS-6 due to its topography and exposure to snowstorms or ice crystals directly affecting the sensor. The absence of similar snow-induced pressure peaks in SS-18 suggests that wind redistribution and topography prevent this effect, except for the peak on May 24th. Major flood peaks (Fe1 to Fe5) were identified in both WS-6 and SS-18 during the warm season, often coinciding with rapid increases in temperature. A particularly high-pressure peak (4500 PSI, 9 November 2022) in WS-6 may be linked to a glacial lake outburst event, supported by observations from the Limnopolar Lake. Outburst floods from lakes could be an important source of sediment supply and channel evolution. In addition, an outburst that does not imply lake failure can also occur, such as snow and ice tunnel collapse, producing lake filling or rapid emptying. This process has been demonstrated to be frequent; however, it has never before recorded by a level sensor on BP. In this case, further analysis is required to confirm whether such events are snowmelt-driven or result from sudden glacial lake drainage. We believe that extraordinary events may play an important role in channel reshaping and size that needs to be further explored in the future.

Water-level variations driven by rising air and soil temperatures, which enhance glacier and permafrost-soil melt, promote adjustments in stream channels. However, the relationship among these factors is complex because, within such a small area, streams fed by glacier melt coexist with others sustained primarily by precipitation or by snowmelt and active-layer water from permafrost. We interpret that a continuous water supply favors the development of larger channels (high bankfull channel dimensions), whereas glacier retreat reduces runoff and leads to channel stabilization, resulting in smaller basins and misfit morphologies. Within this model, additional changes arise from headwater lakes that occasionally produce glacial outburst floods, creating anomalous morphologies (in this case here termed outliers) that deviate from the evolutionary trends observed in the other tributaries (see Fig. 5). Fluvial-network evolution initiates earlier in the western basins, strongly influenced by moist air masses that predominantly enter Byers Peninsula from the west, which explains why the largest basins occur in this sector and why the cluster-like pattern breaks down (Fig. 5): large basins expand at the expense of smaller ones, and in some cases (e.g., WS-6) lake-related catastrophic events further alter normal adjustments. A similar, though less pronounced, pattern is observed in the southern basins, where the largest channels (SS-1 and SS-5) diverge from the cluster's evolutionary trend controlled mainly by soil water and snowmelt contributions. In the northern basins, evolutionary changes are more limited, except for the current meltwater collector of Rotch Dome glacier; because NS-3 is glacier-fed, it also departs from the behavior of the other tributaries (Figs. 4 and 5).

BP streams exhibit different levels of equilibrium. Some of the larger streams show direct relationships between increasing drainage area and increasing channel dimensions. This is in line with the steady-state concept of Park (1978) and the hydraulic-geometry scaling relations suggested by Phillips et al. (2022). However, we observed other streams in which the dimensions do not follow these models. For example, SS-A displayed high A despite the small basin area and dry conditions, indicating a misfit stage caused by rapid glacier retreat. We interpret that this type of stream is the result of a rapid retreat of the glacier that feeds them, and due to a lack of water supply, they are left in a misfit form. In some of these channels, the unbalanced dimensions show recent changes associated with extraordinary lake outburst (Fig. 4).

Downstream hydraulic geometry variables are related to areal geometric progressions (Woldenberg, 1966). This statement has important implications in recent ice-free areas of Polar Regions because it means that we have been able to infer the nature and degree of recent deglaciation processes from the channel morphology of stream systems. We found more evolved streams in the Western basins, related to more warm and moist winds and rains from west to east, probably linked to the influence of LAB (Van Loon, 1967; González et al., 2018). Some morphological characteristics (W/D ratio, A, others) of southern and northern streams are related to slope values. However, the most evolved stream (NS-3) in terms of channel development is located near glacier; therefore, this implies a long stability period in Rotch Dome Glacier, with a continuous water supply in NS-3.

Present and relict morphologies provide insights into past deglaciation and serve as indicators of future changes in the SSI. Misfit streams, such as WS-6, which has a disproportionately wide and high-capacity channel for its estimated A (65.3 m^2), suggest shifts in stream evolution, likely from transient glacier stability during retreat. The presence of paired streams in both northern and southern basins indicates stable phases with continuous meltwater supply as the glacier retreated from west to east. This is consistent with findings by Mink et al. (2014) and Oliva et al. (2016), where interpretations and dating of the deglaciation history can be combined with our results as shown in Fig. 10. The largest basins (NS-9/SS-14, SS-1/NS-8, SS-5/NS-11, WS-7/NS-10) suggest prolonged meltwater activity, while smaller paired basins between them indicate rapid retreat. Only a few large basins (WS-2, WS-4, WS-6) drain westward, shaped by topography and glacial history constraints.

Glacier retreat was complex over time and led to different areas where retreat took place with separation into local glacial centers such as the Ray Promontory in the NW, Chester Cone in the central part of BP, and the still existing Rotch Dome Glacier to the East (Martínez de Pisón et al., 1996; Mink et al., 2014). However, glacier oscillations with advances and retreat of the glacier fronts most likely adds to the complexity of the drainage system influencing the evolution of the stream channels and associated periglacial, paraglacial and fluvial landforms. The fluvial morphological patterns contribute to enhance our

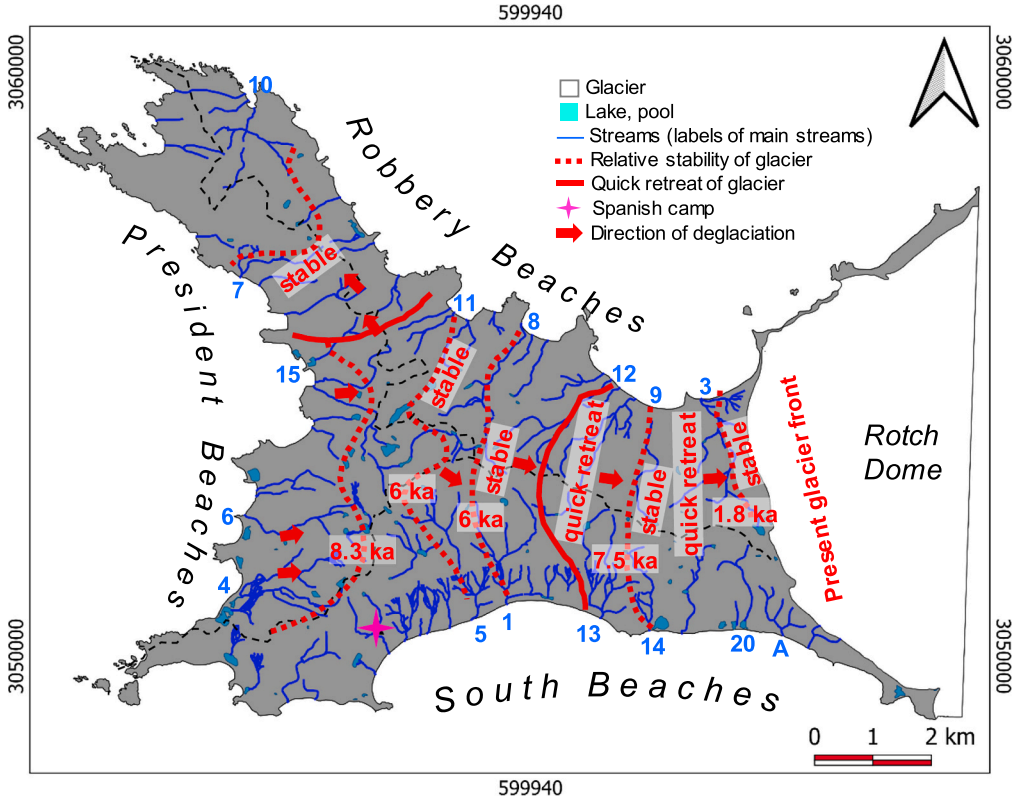

Fig. 10. Hypothetic deglaciation pattern (red arrows) related to stream morphology and size, with periods of relative stability of glacier and quick retreat of the glacier front. The satellite image is from the Copernicus Sentinel-2 mission acquired on the 23rd March 2023) with the fluvial network from López-Martínez et al. (1996a), stream number labelling according to Mink et al. (2014), letter labelling showing additional streams studied in this work and lakes ages from Oliva et al. (2016).

understanding of BP deglaciation and provide a framework for monitoring hydrological changes in response to ongoing climate variability.

6. Conclusions

Seven main morphotypes along the stream channels were identified: Diffuse drainage, lakes in upper platforms, braided systems downstream of lakes and snow patches, canyons, open braided systems on raised beaches, entrenched sections on raised beaches, lagoons and deltas. The morphometric analysis carried out in this study indicates significant variability in channel size, width-to-depth ratios, and other key parameters across different sub-basins. The SS exhibit channels with greater capacity, being wider and deeper. Their steeper slopes suggest higher energy conditions, contributing to more pronounced channel shaping. In contrast, the WS have larger basin areas, indicating a more advanced stage of fluvial system development. This is consistent with their higher stream orders and with the fact that the western coast hosts the highest concentration of large stream basins across the BP region. This pattern likely reflects the direction of deglaciation in BP, progressing from west to east. The R^2 values of the different stream groups in the BP area show good model fits, which improve significantly, when outlier interference is removed. This suggests, on one hand, that normal fluvial evolution processes are strongly controlled by stream orientation and glacier retreat dynamics, and on the other hand, that lake outburst and in some cases snow and ice patches and tunnel collapse events play a significant role in the overall morphological development of the fluvial systems. We interpret the results as a complex evolution of the channels, where basin orientation, glacier proximity and topography are key drivers for channel dimensions. However, the extraordinary events from glacial lake outbursts significantly impact channel morphology and sediment transport. Data recorded by pressure sensors indicated two clear seasonal patterns in water levels, with distinct cold and warm seasons. Peaks in water level pressure were associated with both snow accumulation and flood events.

The streamflow period in the SSI is significantly longer than in other Antarctic regions due to the peculiar climatic conditions, reaching up to six months. Increases in stream discharge can result from both liquid precipitation, which is frequent during the SSI's austral summer, and sudden rises in air temperature that enhance snowmelt. The sensors also recorded extraordinary events associated with glacial lake outbursts, indicating that such processes possibly occur with relative frequency and produce peak flows that are an order of magnitude greater than those generated only by rainfall or snowmelt. This study suggests that many streams in BP are still in a misfit evolutionary stage due to rapid glacier retreat. This results in oversized channels relative to their watershed size, indicating ongoing adjustments in the drainage network. The largest basins indicate prolonged meltwater activity, while smaller and west-draining basins reflect rapid retreat and topographic control. The presence of paired channels in streams along both the northern and southern coasts, exhibiting similar dimensions and morphometric parameters, confirms that the glacial retreat of Rotch Dome occurred from west to east. This retreat progressed in pulses, where periods of stagnation led to the formation of wider and deeper channels, as well as more developed and broader basins. In contrast, episodes of rapid retreat resulted in smaller streams and morphologically narrower channels associated with less evolved and smaller basins.

The fluvial morphological patterns contribute to enhance our understanding of BP deglaciation and provide a framework for monitoring hydrological changes in response to ongoing climate variability. Ongoing research is needed to further understand the complex dynamics of streams within the individual catchment areas and to monitor both seasonal changes and extraordinary events over long periods.

CRediT authorship contribution statement

José Antonio Ortega-Becerril: Writing – review & editing, Writing – original draft, Visualization, Validation, Supervision, Software, Resources, Methodology, Investigation, Formal analysis, Data curation, Conceptualization. **Thomas Schmid:** Writing – review & editing, Writing – original draft, Supervision, Project administration, Methodology, Investigation, Funding acquisition, Formal analysis, Conceptualization. **Juan Pablo Corella:** Writing – review & editing, Writing – original draft, Project administration, Funding acquisition. **Luis Carcavilla:** Writing – review & editing, Writing – original draft, Investigation, Data curation. **Mikel Calle:** Writing – review & editing, Writing – original draft. **Jerónimo López-Martínez:** Writing – review & editing, Writing – original draft, Visualization, Supervision, Methodology, Investigation, Formal analysis, Data curation, Conceptualization.

Declaration of competing interest

The authors declare that they have no known competing financial interests or personal relationships that could have appeared to influence the work reported in this paper.

Acknowledgements

This work was supported by the Projects RTI2018-098099-B-I00 and PID2021-125778OB-I00 of the Spanish R&D National Plan. The authors acknowledge the logistic support provided by the National Antarctic Program of Spain.

Data availability

Data will be made available on request.

References

Abram, N.J., Mulvaney, R., Wolff, E.W., Triest, J., Kipfstuhl, S., Trusel, L.D., Arrowsmith, C., 2013. Acceleration of snowmelt in an Antarctic Peninsula ice core during the twentieth century. Nat. Geosci. 6 (5), 404. https://doi.org/10.1038/NGEO1787.

Antarctic Treaty Secretariat, 2022. Antarctic Specially Protected Area No. 126 (Byers Peninsula, Livingston Island, South Shetland Islands): Revised Management Plan.

Bañón, M., 2001. Observaciones meteorológicas en la Base Antártica Española Juan Carlos I. Instituto Nacional de Meteorología, Madrid. Monografía, A151, 135 pp.

Bañón, M., Justel, A., Velázquez, D., Quesada, A., 2013. Regional weather survey on Byers Peninsula, Livingston Island, South Shetland Islands, Antarctica. Antarctic Science 25 (2), 146–156. https://doi.org/10.1017/S0954102012001046.

Baroni, C., Noti, V., Ciccacci, S., Righini, G., Salvatore, M.C., 2005. Fluvial origin of the valley system in northern Victoria Land (Antarctica) from quantitative geomorphic analysis. Geol. Soc. Am. Bull. 117 (1–2), 212–228. https://doi.org/10.1130/B25529.1.

Barsch, D., Mäusbacher, R., 1986. New data on the relief development of the South Shetland Islands, Antarctica. Interdiscip. Sci. Rev. 11, 211–218. https://doi.org/10.1016/j.quascirev.2011.07.021.

Bendixen, M., Lønsmann Iversen, L., Anker Bjørk, A., Elberling, B., Westergaard-Nielsen, A., Overeem, I., Barnhart, K.R., Khan, S.A., Box, J.E., Abermann, J., Langley, K., Kroon, A., 2017. Delta progradation in Greenland driven by increasing glacial mass loss. Nature 550 (7674), 101–104. https://doi.org/10.1038/nature23873.

Birnie, R.V., Gordon, J.E., 1980. Drainage systems associated with snow melt, South Shetland Islands, Antarctica. Geogr. Ann. Ser. B 62 (1–2), 57–62. https://doi.org/10.2307/520452.

Björck, S., Zale, R., 1996. Late Holocene tephrochronology and palaeoclimate, based on lake sediment studies. In: López-Martínez, J., Thomson, M.R.A., Thomson, J.W. (Eds.), Geomorphological Map of Byers Peninsula, Livingston Island, Geomap Series, 5-A. British Antarctic Survey, Cambridge, pp. 43–48 with supplementary text.

Björck, S., Hakansson, H., Zale, R., Karlén, W., Jönsson, B.L., 1991. A late Holocene lake sediment sequence from Livingston Island, South Shetland Islands, with palaeoclimatic implications. Antarct. Sci. 3, 61–72. https://doi.org/10.1017/S095410209100010X.

Björck, S., Hakansson, H., Olsson, S., Barnekow, L., Janssens, J., 1993. Palaeoclimatic studies in South Shetland Islands, Antarctica, based on numerous stratigraphic variables in lake sediments. J. Paleolimnol. 8, 233–272. https://doi.org/10.1007/BF00177858.

Björck, S., Hjort, C., Ingolfsson, O., Zale, R., Ising, J., 1996. Holocene deglaciation chronology from lake sediments. In: López-Martínez, J., Thomson, M.R.A., Thomson, J.W. (Eds.), Geomorphological Map of Byers Peninsula, Livingston Island, Geomap Series, 5-A. British Antarctic Survey, Cambridge, pp. 49–51 with supplementary text.

Bockheim, J., Vieira, G., Ramos, M., López-Martínez, J., Serrano, E., Guglielmin, M., Wilhelm, K., Nieuwendam, A., 2013. Climate warming and permafrost dynamics in the Antarctic Peninsula region. Global Planet. Change 100, 215–223. https://doi.org/10.1016/j.gloplacha.2012.10.018.

Conovitz, P.A., McKnight, D.M., MacDonald, L.H., Fountain, A.G., House, H.R., 1998. Hydrologic processes influencing streamflow variation in Fryxell Basin, Antarctica. In: Priscu, J.C. (Ed.), Ecosystem Dynamics in a Polar Desert: The McMurdo Dry Valleys, Antarctica, Antarctic Research Series, 72, pp. 93–108. https://doi.org/10.1029/AR072p0093.

Convey, P., Chown, S.L., Clarke, A., Barnes, D.K.A., Bokhorst, S., Cummings, V., Ducklow, H.W., Frati, F., Green, A.T.G., Gordon, S., Griffiths, H.J., Howard-Williams, C., Huiskes, A.J.L., Laybourn-Parry, J., Lyons, W.B., McMinn, A., Morley, S.A., Peck, L.S., Quesada, A., Robinson, S.A., Schiaparelli, S., Wall, D.H., 2014. The spatial structure of Antarctic biodiversity. Ecological monographs 84 (2), 203–244. https://doi.org/10.1890/12-2216.1.

Cuchí, J.A., Durán, J.J., Alfaro, P., Serrano, E., López-Martínez, J., 2004. Discriminación mediante parámetros físicoquímicos "in situ", de diferentes tipos de agua presentes en un área con permafrost (península Byers, isla Livingston, Antártida Occidental). Boletín de la Real Sociedad Española de Historia Natural. Sección Geológica 99 (1), 75–82.

De Pablo, M.A., Ramos, M., Molina, A., 2014. Thermal characterization of the active layer at the Limnopolar Lake CALM-S site on Byers Peninsula (Livingston Island), Antarctica. Solid Earth 5 (2), 721–739. https://doi.org/10.5194/se-5-721-2014.

De Pablo, M.A., Ramos, M., Molina, A., 2017. Snow cover evolution, on 2009-2014, at the Limnopolar Lake CALM-S site on Byers Peninsula, Livingston Island, Antarctica. Catena 149, 538–547. https://doi.org/10.1016/j.catena.2016.06.002.

De Pablo, M.A., Ramos, M., Vieira, G., Molina, A., Ramos, R., Maior, C.N., Prieto, M., Ruiz-Fernández, J., 2023. Interannual variability of ground surface thermal regimes in Livingston and Deception islands, Antarctica (2007–2021). Land Degrad. Dev. 35 (1), 378–393. https://doi.org/10.1002/ldr.4922.

Falk, U., Silva-Busso, A., Pölcher, P., 2018. A simplified method to estimate the run-off in Periglacial Creeks: a case study of King George Islands, Antarctic Peninsula. Philos. T. Roy. Soc. Am. 376, 20170166. https://doi.org/10.1098/rsta.2017.0166.

Ferreira, A., Vieira, G., Ramos, M., Nieuwendam, A., 2017. Ground temperature and permafrost distribution in Hurd Peninsula (Livingston Island, Maritime Antarctic): an assessment using freezing indexes and TTOP modelling. Catena 149, 560–571. https://doi.org/10.1016/j.catena.2016.08.027.

González, S., Vasallo, F., Recio-Blitz, C., Guijarro, J.A., Riesco, J., 2018. Atmospheric patterns over the Antarctic Peninsula. J. Climate 31 (9), 3597–3608. https://doi.org/10.1175/JCLI-D-17-0598.1.

Gooseff, M.N., McKnight, D.M., Runkel, R.L., Vaughn, B.H., 2003. Determining long time-scale hyporheic zone flow paths in Antarctic streams. Hydrol. Process. 17 (9), 1691–1710. https://doi.org/10.1002/hyp.1210.

Hall, B.L., 2009. Holocene glacial history of Antarctica and the sub-Antarctic islands. Quat. Sci. Rev. 28, 2213–2230. https://doi.org/10.1016/j.quascirev.2009.06.011.

Hall, B.L., Perry, E.R., 2004. Variations in ice rafted detritus on beaches in the South Shetland Islands: a possible climate proxy. Antarct. Sci. 16 (3), 339–344. https://doi.org/10.1017/S0954102004002147.

Inbar, M., 1995. Fluvial morphology and streamflow on Deception Island, Antarctica. Geogr. Ann. Ser. B 77 (4), 221–230. https://doi.org/10.1080/04353676.1995.11880442.

John, B.S., Sugden, D.E., 1971. Raised marine features and phases of glaciation in the South Shetland Islands. British Antarctic Survey Bulletin 24, 45–111.

Kavan, J., 2022. Fluvial transport in the deglaciated Antarctic catchment–Bohemian Stream, James Ross Island. Geogr. Ann. Ser. B 104 (1), 1–10. https://doi.org/10.1080/04353676.1995.11880442.

Kavan, J., Ondruch, J., Nývlt, D., Hrbáček, F., Carrivick, J.L., Láska, K., 2017. Seasonal hydrological and suspended sediment transport dynamics in proglacial streams, James Ross Island, Antarctica. Geogr. Ann. Ser. B 99 (1), 38–55. https://doi.org/10.1080/04353676.2016.1257914.

Kejna, M., 2003. Trends of Air Temperature of the Antarctic during the period 1958–2000. Polish Polar Research 24, 99–126.

Khim, B.K., Shim, J., Yoon, H.I., Kang, Y.C., Jang, Y.H., 2007. Lithogenic and biogenic particle deposition in an Antarctic coastal environment (Marian Cove, King George Island): Seasonal patterns from a sediment trap study. Estuar. Coast. Shelf Sci. 73 (1–2), 111–122. https://doi.org/10.1016/j.ecss.2006.12.015.

King, J.C., Turner, J., 1997. Antarctic Meteorology and Climatology. Cambridge University Press, Cambridge. https://doi.org/10.1017/CBO9780511524967, 409 pp.

Lecomte, K.L., Vignoni, P.A., Cordoba, F.E., Chaparro, M.A.E., Kopalova, K., Gargiulo, J. D., Lirio, J.M., Irurzun, M.A., Böhnel, H.N., 2016. Hydrological systems from the Antarctic Peninsula under climate change: James Ross archipelago as study case. Environ. Earth Sci. 75 (623), 1–20. https://doi.org/10.1007/s12665-016-5406-y.

Leopold, L.B., Maddock, T., 1953. The Hydraulic Geometry of Stream Channels and Some Physiographic Implications. U.S. 548 Geol. Surv. Prof. Pap., 252. https://doi.org/10.3133/pp252.

Leopold, L.B., Wolman, M.G., Miller, J.P., 1964. Fluvial Processes in Geomorphology. Freeman and Co., San Francisco, 522 pp.

Li, D., Lu, X., Overeem, I., Walling, D.E., Syvitski, J., Kettner, A.J., Bookhagen, B., Zhou, Y., Zhang, T., 2021. Exceptional increases in fluvial sediment fluxes in a warmer and wetter High Mountain Asia. Science 374 (6567), 599–603. https://doi.org/10.1126/science.abi9649.

López-Martínez, J., Martínez de Pisón, E., Serrano, E., Arche, A., 1996a. Geomorphological map of Byers Peninsula, Livingston Island. E. 1:25,000. In: López-Martínez, J., Thomson, M.R.A., Thomson, J.W. (Eds.), Geomorphological map of Byers Peninsula, Livingston Island, BAS Geomap Series, Sheet 5-A. British Antarctic Survey, Cambridge.

López-Martínez, J., Serrano, E., Martínez de Pisón, E., 1996b. Geomorphological features of the drainage system. In: López-Martínez, J., Thomson, M.R.A., Thomson, J.W. (Eds.), Geomorphological map of Byers Peninsula, Livingston Island, BAS Geomap Series, Sheet, 5-A. British Antarctic Survey, Cambridge, pp. 15–22 with supplementary text.

López-Martínez, J., Thomson, M.R.A., Thomson, J.W., 1996c. Geomophological Map of Byers Peninsula, Livingston Island. In: BAS Geomap Series, Sheet 5-A. British Antarctic Survey, Cambridge, 65 pp. + 2 maps.

López-Martínez, J., Serrano, E., Schmid, T., Mink, S., Linés, C., 2012. Periglacial processes and landforms in the South Shetland Islands (northern Antarctic Peninsula region). Geomorphology 155, 62–79. https://doi.org/10.1016/j.geomorph.2011.12.018.

Martínez de Pisón, E., Serrano, E., Arche, A., López-Martínez, J., 1996. Glacial geomorphology. In: López-Martínez, J., Thomson, M.R.A., Thomson, J.W. (Eds.), Geomorphological Map of Byers Peninsula, Livingston Island. British Antarctic Survey, Cambridge (UK), pp. 23–27.

Mink, S., López-Martínez, J., Maestro, A., Garrote, J., Ortega, J.A., Serrano, E., Durán, J. J., Schmid, T., 2014. Insights into deglaciation of the largest ice-free area in the South Shetland Islands (Antarctica) from quantitative analysis of the drainage system. Geomorphology 225, 4–24. https://doi.org/10.1016/j.geomorph.2014.03.028.

Molina, C., Navarro, F.J., Calvet, J., García-Sellés, D., Lapazarán, J.J., 2007. Hurd Peninsula glaciers, Livingston Island, Antarctica, as indicators of regional warming: ice-volume changes during the period 1956–2000. Ann. Glaciol. 46, 43–49. https://doi.org/10.3189/172756407782871765.

Navarro, F.J., Jonsell, U.Y., Corcuera, M.I., Martín-Español, A., 2013. Decelerated mass loss of Hurd and Johnsons Glaciers, Livingston Island, Antarctic Peninsula. J. Glaciol. 59, 115–128. https://doi.org/10.3189/2013JoG12J144.

Oliva, M., Antoniades, D., Giralt, S., Granados, I., Pla-Rabes, S., Toro, M., Liu, E.J., Sanjurjo, J., Vieira, G., 2016. The Holocene deglaciation of the Byers Peninsula (Livingston Island, Antarctica) based on the dating of lake sedimentary records. Geomorphology 261, 89–102. https://doi.org/10.1016/j.geomorph.2016.02.029.

Oliva, M., Navarro, F., Hrbáček, F., Hernández, A., Nývlt, D., Pereira, P., Ruiz-Fernández, J., Trigo, R., 2017. Recent regional climate cooling on the Antarctic Peninsula and associated impacts on the cryosphere. Geomorphology 261, 89–102. https://doi.org/10.1016/j.geomorph.2016.02.029.

Palacios, D., Ruiz-Fernández, J., Oliva, M., Andrés, N., Fernández-Fernández, J.M., Schimmelpfennig, I., Leanni, L., González-Díaz, B., Aster Team, 2020. Timing of formation of neoglacial landforms in the South Shetland Islands (Antarctic Peninsula): Regional and global implications. Quat. Sci. Rev. 234, 106248. https://doi.org/10.1016/j.quascirev.2020.106248.

Park, C.C., 1978. Allometric analysis and stream channel morphometry. Geogr. Anal. 10 (3), 211–228. https://doi.org/10.1111/j.1538-4632.1978.tb00651.x.

Phillips, C.B., Masteller, C.C., Slater, L.J., Dunne, K.B., Francalanci, S., Lanzoni, S., Jerolmack, D.J., 2022. Threshold constraints on the size, shape and stability of alluvial rivers. Nat. Rev. Earth Environ. 3 (6), 406–419. https://doi.org/10.1038/s43017-022-00282-z.

Pla-Rabes, S., Toro, M., Van de Vijver, B., Rochera, C., Villaescusa, J.A., Camacho, A., Quesada, A., 2013. Stability and endemicity of benthic diatom assemblages from different substrates in a maritime stream on Byers Peninsula, Livingston Island, Antarctica: the role of climate variability. Antarct. Sci. 25 (2), 254–269. https://doi.org/10.1017/S0954102012000922.

Quintana, J., Carrasco, J.F., 2000. Temperature and precipitation behavior during 1961–1998 period at the northern tip of the Antarctic Peninsula. In: Sixth International Conference on Southern Hemisphere Meteorology and Oceanography. Amer. Meteo. Soc., pp. 234–235.

Ramos, M., Vieira, G., de Pablo, M.A., Molina, A., Abramov, A., Goyanes, G., 2017. Recent shallowing of the thaw depth at Crater Lake, Deception Island, Antarctica (2006–2014). Catena 149 (2), 519–528. https://doi.org/10.1016/j.catena.2016.07.019.

Rau, F., Braun, M., 2002. The regional distribution of the dry-snow zone on the Antarctic Peninsula north of 70° S. Ann. Glaciol. 34, 95–100. https://doi.org/10.3189/172756402781817914.

Rochera, C., Justel, A., Fernández-Valiente, E., Bañón, M., Rico, E., Toro, M., Camacho, A., Quesada, A., 2010. Interannual meteorological variability and its effects on a lake from maritime Antarctica. Polar Biol. 33, 1615–1628. https://doi.org/10.1007/s00300-010-0879-8.

Ruiz-Fernández, J., Oliva, M., 2016. Relative palaeoenvironmental adjustments following deglaciation of the Byers Peninsula (Livingstone Island, Antarctica). Arct. Antarct. Alp. Res. 48 (2), 345–359. https://doi.org/10.1657/AAAR0015-014.

Ruiz-Fernandez, J., Oliva, M., Nyvlt, D., Cannone, N., Garcia-Hernandez, C., Guglielmin, M., Hrbaček, F., Roman, M., Fernández, S., López-Martínez, J., Antoniades, D., 2019. Patterns of spatio-temporal paraglacial response in the Antarctic Peninsula region and associated ecological implications. Earth Sci. Rev. 192, 379–402. https://doi.org/10.1016/j.earscirev.2019.03.014.

Serrano, E., Martínez de Pisón, E., López-Martínez, J., 1996. Periglacial and nival landforms and deposits. In: López-Martínez, J., Thomson, M.R.A., Thomson, J.W. (Eds.), Geomorphological Map of Byers Peninsula, Livingston Island, Geomap Series, 5-A. British Antarctic Survey, Cambridge, pp. 28–34 with supplementary text.

Serrano, E., López-Martínez, J., Cuchí, J.A., Durán, J.J., Mink, S., Navas, A., 2008. Permafrost in the South Shetland Islands (maritime Antarctica): spatial distribution pattern. In: Kane, D.L., Hindel, K.M. (Eds.), Proceedings Ninth International Conference on Permafrost Institute of Northern Engineering, 2. University of Alaska, Fairbanks, pp. 1621–1625.

Shahateet, K., Seehaus, T., Navarro, F., Sommer, C., Braun, M., 2021. Geodetic Mass Balance of the South Shetland Islands Ice Caps, Antarctica, from Differencing TanDEM-X DEMs. Remote Sens. 13 (17), 3408. https://doi.org/10.3390/rs13173408.

Simmonds, I., Keay, K., Lim, E., 2003. Synoptic activity in the seas around the Antarctic. Mon. Weather Rev. 131, 272–288. https://doi.org/10.1175/1520-0493(2003)131<0272:SAITSA>2.0.CO;2.

Sone, T., Fukui, K., Strelin, J.A., Torielli, C.A., Mori, J., 2007. Glacier lake outburst flood on James Ross Island, Antarctic Peninsula region. Pol. Polar Res. 28, 3–12.

Steig, E.J., Schneider, D.P., Rutherford, S.D., Mann, M.E., Comiso, J.C., Shindell, D.T., 2009. Warming of the Antarctic ice-sheet surface since the 1957 International Geophysical Year. Nature 457 (7228), 459–462. https://doi.org/10.1038/nature07669.

Thomson, M.R.A., López-Martínez, J., 1996. Introduction. In: López-Martínez, J., Thomson, M.R.A., Thomson, J.W. (Eds.), Geomorphological Map of Byers Peninsula, Livingston Island, BAS Geomap Series, Sheet, 5-A. British Antarctic Survey, Cambridge, pp. 1–4 with supplementary text.

Toro, M., Camacho, A., Rochera, C., Rico, E., Bañón, M., Fernández-Valiente, E., Marco, E., Justel, A., Avendaño, M.C., Ariosa, Y., Vincent, W.F., Quesada, A., 2007. Limnological characteristics of the freshwater ecosystems of Byers Peninsula, Livingston Island, in maritime Antarctica. Polar Biol. 30, 635–649. https://doi.org/10.1007/s00300-006-0223-5.

Toro, M., Granados, I., Pla, S., Giralt, S., Antoniades, D., Galán, L., Appleby, P.G., 2013. Chronostratigraphy of the sedimentary record of Limnopolar lake, Byers Peninsula, Livingston Island, Antarctica. Antarct. Sci. 25 (2), 198–212. https://doi.org/10.1017/S0954102012000788.

Turner, J., Colwell, S.R., Marshall, G.J., Lachlan-Cope, T.A., Carleton, A.M., Jones, P.J., Lagun, V., Reid, P.A., Iagovkina, S., 2004. The SCAR READER Project. Toward a high quality database of mean Antarctic meteorological observations. J. Climate 17, 2890–2898. https://doi.org/10.1175/1520-0442(2004)017.

Turner, J., Lu, H., White, I., King, J.C., Phillips, T., Hosking, J.S., Bracegirdle, T.J., Marshall, G.J., Mulvaney, R., Deb, P., 2016. Absence of 21st century warming on Antarctic Peninsula consistent with natural variability. Nature 535. https://doi.org/10.1038/nature18645.

Van Loon, H., 1967. The half-yearly oscillations in middle and high southern latitudes and the coreless winter. J. Atmos. Sci. 24 (5), 472–486. https://doi.org/10.1175/1520-0469(1967)024<0472:THYOIM>2.0.CO;2.

Vaughan, D.G., Marshall, G., Connolley, W.M., Parkinson, C., Mulvaney, R., Hodgson, D. A., King, J.C., Pudsey, C.J., Turner, J., Wolff, E., 2003. Recent rapid regional climate warming on the Antarctic Peninsula. Clim. Change 60, 243–274. https://doi.org/10.1023/A:1026021217991.

Vieira, G., Bockheim, J., Guglielmin, M., Balks, M., Abramov, A.A., Boelhouwers, J., Cannone, N., Ganzert, L., Gilichinsky, D.A., Goryachkin, G., López-Martínez, J., Meiklejohn, J., Raffi, R., Ramos, M., Schaefer, C., Serrano, E., Simas, F., Sletten, R., Wagner, D., 2010. Thermal state of permafrost and active-layer monitoring in the Antarctic: advances during the International Polar Year 2007–2009. Permafr. Periglac. Process. 21, 182–197. https://doi.org/10.1002/ppp.685.

Wohl, E., 2020. Rivers in the Landscape. John Wiley & Sons, 318 pp.

Woldenberg, M.J., 1966. Horton's laws justified in terms of allometric growth and steady state in open systems. Geol. Soc. Am. Bull. 77 (4), 431–434. https://doi.org/10.1130/0016-7606(1966)77[431:HLJITO]2.0.CO;2.

Wolman, M.G., Leopold, L.B., 1957. River Flood Plains: Some Observations on Their Formation. Geological Survey Professional Paper, 282-C,. U.S. Government Printing Office, Washington DC, pp. 87–109. https://doi.org/10.3133/pp282C.

Woo, M., 2012. Permafrost Hydrology. Springer. https://doi.org/10.1007/978-3-642-23462-0, 563 pp.

Zwoliński, Z., 2007. The Mobility of Mineral Matter in Paraglacial Areas. King George Island, Western Antarctica. In: Seria Geografia, 74. Adam Mickiewicz University Press, 266 pp. ISBN 978-83-232172-4-4. ISSN 0554-8128. Text in Polish with a summary in English.

Zwoliński, Z., Kejna, M., Rachlewicz, G., Sobota, I., Szpikowski, J., 2016. Solute and sedimentary fluxes on King George Island. In: Beylich, A.A., Dixon, J.C., Zwoliński, Z. (Eds.), Source-to-Sink Fluxes in Undisturbed Cold Environments. Cambridge University Press, pp. 213–237.